N-70-CR
33435
871

PFC/RR-91-2

MIT ASTROMAG 1.7 METER DISK MAGNET DESIGN REPORT

P.G. Marston, J.R. Hale, R. Vieira, A. Zhukovsky,
P.H. Titus, J.D. Sullivan, A.M. Dawson

January 1990

Plasma Fusion Center
Massachusetts Institute of Technology
Cambridge, Massachusetts 02139 USA

This work was supported by the U.S. NASA under NASA Grant #5-1106

MIT ASTROMAG 1.7 METER DISK MAGNET DESIGN REPORT

DECEMBER 28, 1990

**P.G. Marston, J.R. Hale, R. Vieria, A. Zhukovsky,
P.H. Titus, J.D. Sullivan, A.M. Dawson**

INTRODUCTION

MIT has proposed a magnet design for ASTROMAG, which has demonstrated substantial improvement in performance as compared with the present (HEAO) baseline design. This work has been reported previously and presented at a NASA review May 15-17, 1990. The work presented herein covers that performed during the period June-December 1990, and is generally a response to concerns, criticisms etc., that were raised during the NASA review. Several advantages of the MIT disk design are listed below, Tables 1 and 2 give the design characteristics while Figs. 1-9 show details of field contours and active field regions, as well as comparisons with other designs.

ADVANTAGES

Structural Integrity

- Lower Hoop Stresses (Lower $J\lambda$, Lower R x B)
- Lighter, Stronger, Stiffer support material
- Optimized distribution of support material
- 50% cross section for equivalent stress
- High Quality Winding Composite
- No Force Containment Structure Required (no related structural requirement)

Stability

Related to Structural Integrity / Thermal Perturbations
Lower Strain / Better Suited to High Purity Aluminum
Lower ratio of I_{op}/I_c / Design Approach Permits Optimization of Radial Current Distribution to Further Reduce Peak Fields (Except $B_{max} < 6$ T)

DESCRIPTIONS OF ALTERNATIVE DESIGN CONCEPTS

Three alternative design configurations for the ASTROMAG disk coils are summarized herein. Table 1 lists the parameters of the conductors proposed for the three; Table 2 shows basic parameters for each of the complete systems. The chief distinguishing features of the three are summarized below.

Configuration V10, the MIT Baseline Concept

- The coils are manufactured as monolithic high-pressure laminates
- The conductor is a circular cross section, copper/NbTi wire
- Three winding regions, all with the same OD, but different IDs
- Overall current density within each region is constant, and is the same in all three configurations
- Operating current is 1200 A, about 50% of critical
- Provisions for two quench-back layers, to be either aluminum wire spirals or thin aluminum disks

- The winding distribution places more of the total NI at locations closer to the detector volume; the finished package presents a full-diameter flat surface toward the detector space

- Magnet system would have the capability to be operated at any desired energy level up to a maximum of more than 22 MJ

Configuration V18, the Aluminum-stabilized Conductor Version

- The coils are manufactured as a potted stack of double pancakes

- The conductor is a rectangular cross section aluminum/ copper/NbTi composite

- Three primary winding regions, all with the same OD, but different IDs; there is a small radial extent of higher pitch winding at the ID of two of the primary regions

- Overall current density within each primary region is constant, and the same in all three; diminished current density in the two subregions described above

- Operating current is 1000 A, about 44% of critical

- Provision for three quench-back rings, one nested at the ID of each of the winding regions

- The winding distribution places more of the total NI at locations closer to the detector volume; the finished package presents a full-diameter flat surface toward the detector space

- Magnet system would have the capability to be operated at any desired energy level up to a maximum of more than 25 MJ

Configuration R5, the Variable Pitch Concept

- The coils are manufactured as monolithic high-pressure laminates
- The conductor is a circular cross section, copper/NbTi wire
- A single, constant-thickness disk-shaped winding region, in which the winding pitch is a decreasing function of radius
- Overall current density is a minimum at the ID, and increases with radius to a maximum at the OD
- Operating current is 300 A, about 46% of critical
- Provision for two quench-back layers, to be either aluminum wire spirals or thin aluminum disks
- Magnet system would have the capability to be operated at any desired energy level up to a maximum of more than 23 MJ
- Low operating current reduces losses in energizing circuitry (e.g., power supply, gas-cooled leads). Appendix B contains field plots for all three designs.

A good summary of three different configurations of this design and their advantages is presented in Ref. 1 which is attached as Appendix A. Appendix B contains field plots for all three configurations of this design. The advantages of this design accrue from its overall geometry (winding and current distribution), its structural support scheme, and the proposed method of manufacture.[1] All three configurations take advantage of the fact that the useful field (the experiment) is located external to the magnet bore. The large radial distribution of the windings results in much higher external fields and lower peak fields in the winding. The support structure which bridges the central hole (winding bore) is inherently more efficient than an external support ring by a factor of 2. It is important to understand this advantage when assessing the MIT design on the basis of

stored energy vs weight (in comparison to HEAO and the existing data base). The manufacturing technique is specifically intended to overcome the major cause of failure in epoxy-impregnated magnet coils of this generic type.

REVIEWERS' CONCERNS

High Performance

Both magnets (HEAO and Disk) operate at relatively high magnetic field strengths, average current densities, and stress levels. They both reflect a ratio of stored energy to mass that is substantially higher than any other in the existing data base. This is a legitimate cause for concern and necessitates a substantial manufacturing development and verification test program for either design.

At the design point however, the disk geometry achieves a MDR ratio of 1.61 compared to the HEAO aluminum geometry, and 1.86 compared to the HEAO copper design. This is at equivalent mass and average current density, and at lower peak stress (170 vs 260 MPa) because the magnetic and structural design is more efficient. If this same design is scaled back to equivalent MDR and proper credit is given for its inherent structural efficiency (low stress) then it is in a range of combined stress, current density and stored energy vs mass which is comparable to the existing state-of-the-art. Figure 10 shows the comparative distribution of the peak field in the winding at 13.8 megajoules. The local hoop stress in the winding is the product of the magnetic field times the radius times the current density (BRJ). For the operating conditions shown, the current density of the disk is approximately 75% that of the LBL baseline. Figure 11 demonstrates the very low stresses at this operating point and Fig. 12 shows the comparative field distributions at various axial distances away from the coil face. Tables 3 and 4 tabulate the comparative performance.

Manufacturing Technique

The principal causes of failure for fully impregnated (potted) superconducting magnets are lack of mechanical integrity in the winding

composite and lack of structural integrity between the winding and its support structure. The proposed manufacturing scheme wherein the winding is manufactured as a high pressure laminate with the superconducting wire as a part of the composite is an attempt to achieve internal mechanical perfection and zero hysteresis, and to eliminate the need for additional structure. The winding is its own structure and eliminates such difficult interface failure modes. Several concerns were raised with respect to the fact that this is not a proven technique (the Catch-22 is that the proven techniques have also proven to be very troublesome).

One of these concerns was that the wires would move during the high pressure cure. We have since done a small amount of winding development and have wound a small four-layer superconducting coil. The winding development and X-rays of the small coil do not indicate any problem with wire motion during cure. Although the scale is small with respect to ASTROMAG, it is large with respect to the wire (failure mechanism) and provides a reasonable assurance of large scale success.

Another specific concern of the design relates to quench propagation in a composite wherein the turns of the winding are spaced at a relatively large distance compared to most of the prior art. Quench calculations for reasonable distributions of quench-back windings indicate that protection should not be a problem.

It must also be noted that the high pressure laminate manufacturing technique is not necessary to the implementation of the very efficient electromagnetic and structural design concepts. As an example, we have carried through a design using a two-to-one aspect ratio aluminum stabilized conductor (nearly identical to that considered by both Green and Yamamoto in their aluminum-stabilized coil designs). This design would use a standard pancake winding technique which would also benefit from the general configuration and structural support scheme. The energy margin of the aluminum-stabilized winding is approximately two orders of magnitude greater than that of the copper-stabilized design, but if internal thermal perturbations as a result of mechanical imperfections were equivalently greater, this design would have no comparative merit (another Catch-22). It is worth noting that even with the aluminum

conductor, the local thermal perturbation required to quench the magnet is less than one millijoule per cm^2 of conductor. Considering the size of this magnet, the magnitude of the forces on its support structure, and its more than ten megajoules of stored energy, this is a very small amount of energy. The need for absolute structural perfection is obvious.

High Operating Current

One of the concerns for both designs was the fact that the 1000 ampere operating current imposes a severe energy penalty (related to voltage drop in the power supply) on the space station energy source. Although low current designs become considerably more difficult (and risky) for the conventional layer-wound coil configuration, the automated "wire positioning" technique proposed for the disk magnet is very well suited to the use of small-diameter wire (structural integrity would most likely improve). We have therefore also carried through a 300 ampere design (0.76 millimeter diameter wire) which results in a total disk thickness of only 6.4 centimeters.

REFERENCES

1. P.G. Marston, et al., Design of an Opposing Pair Magnet System for ASTROMAG, presented at the 1990 Applied Superconductivity Conference, Snowmass, CO., September 1990. To be published, IEEE Trans. Mag., March 1991.

Table 1
Conductor Characteristics

	V10	V18	R5
Wire Dimen. (m)	0.00156	0.0016 x 0.00259	0.00076
Corner radius (m)	n.a.	0.0005	n.a.
Insulation Thickness (m)	0.0001	0.0001	0.0001
Al:Cu:sc	0:1.35:1	4:0.8:1	0:1.35:1
Operating Temp. (K)	1.8	1.8	1.8
I_c, 1.8 K, B_{max} (A)	2389	2252	645
I_{op} (A)	1200	1000	300
I_{op}/I_c	0.502	0.44	0.465
T_{cs} (K)	3.87	4.29	4.16
Temp. Margin (K) (T_{cs}-T_b)	2.07	2.49	2.36

Table 2
System Characteristics

Pancake Spiral Pitch	const.	const.	function of radius
Pitch at ID (m)	0.00234	0.0018	0.006
Pitch at OD (m)	0.00234	0.0018	0.0012
Interpancake Separation (m)	0.00321	0.00429	0.00152
Winding Envelope ID (m)	0.40	0.40	0.34
Winding Envelope OD (m)	1.70	1.70	1.70
Winding Envelope Overall Length (m)	0.0684	0.0858	0.0638
Peak Field (T)	7.22	6.64	6.67
Total N	3484	4354	15018
NI (MA)	4.18	4.35	4.505
λJ (max) (10^8 A/m^2)	1.63	1.29	1.61
λj (min) (10^8 A/m^2)	n.a.	n.a	0.329
System Inductance (two coils) (H)	31.5	50.6	513
System Stored Energy, I_{op} (MJ)	22.7	25.3	23.1
I_{op} for 11 MJ Energy (A)	835	659	207
Length of s.c. wire, per coil (m)	1.32e4	1.68e4	5.52e4
Mass of s.c. wire (kg)	193	291	193
Mass of two Al wire pancakes (kg)	8.6	n.a.	3.6
Total wire mass per coil (kg)	201.6	291	197
Mass of Support Structure (kg)	123	73	159
Total Mass of Each Magnet Disk (kg)	325	364	356
Intercoil Repulsive Force (N)	1.225e6	0.634e6	0.582e6

The geometries and field distribution is for these designs are attached as Appendix B.

Comparative Physics Performance scaled with stored energy

Magnet	Stored Energy (MJ)	Average Impulse (T m)
LBL Cu Baseline	11.0	0.92
LBL Al Case 1.	11.0	0.94
LBL Al Case 3.	11.0	0.91
MIT Disk	11.0	1.03
LBL Al Case 1.	13.9	1.05
LBL Al Case 3.	13.9	1.02
MIT Disk	13.9	1.15

TABLE 3: MDM calculations by R. Streimatter (NASA) et al., show a comparative improvement which is approximately 12% greater than that shown by these MIT calculations

Comparative Mass and Physics Performance at the design operating point

Magnet	Mass (kg)	Stored Energy (MJ)	Average Impulse (T m)
LBL Cu Baseline	650	11.0	0.92
LBL Al Case 1.	700	13.9	1.05
LBL Al Case 3.	1100	22.3	1.29
MIT Disk	650	22.3	1.48

TABLE 4: Note that the MIT design is 22.3 MJ design and is thus much more conservative than the baseline in this comparison. A lower energy disk could have substantially lower mass than the LBN baseline. The principal advantage of the MIT design, however, is improved physics at equivalent mass, current density, stress etc. These designs therefore represent optimization for maximum performance at equivalent mass rather than minimum mass at equivalent performance.

COMMENTS ON LAMINATE MANUFACTURE

One of the primary requirements of any ASTROMAG coil design is that the magnet coils must have near-perfect structural integrity. To this end, two of the three designs described herein would be manufactured as a monolithic composite, in which the superconducting wire is incorporated as one of the components. By utilizing a precision X-Y numerically controlled winding machine, the coil would be built up in pancake layers, alternating prepreg sheets of fiber/epoxy (e.g., carbon or kevlar fiber) with a layer of NbTi wire that spirals from OD to ID in one layer, from ID to OD in the next, and so on. Upon completion of the winding, the composite is processed through a curing cycle under high pressure (approximately 200 psi) and vacuum.

The calculated strength of the magnet composite (fiber matrix plus the superconducting wire) is approximately 530 MPa based on a mixture rule. Plans for the testing that will be carried out in order to establish the tensile and interlaminate strength of the magnet composite are currently being formulated, and preliminary talks have been held with a potential vendor for test specimens .

A small coil, representative of design "R5" has been produced with the "multiwire" equipment as a carbon fiber-epoxy high pressure laminate. Visual (including X-ray) inspection indicates complete success. The coil has not, however, been tested. This coil is described in Appendix C.

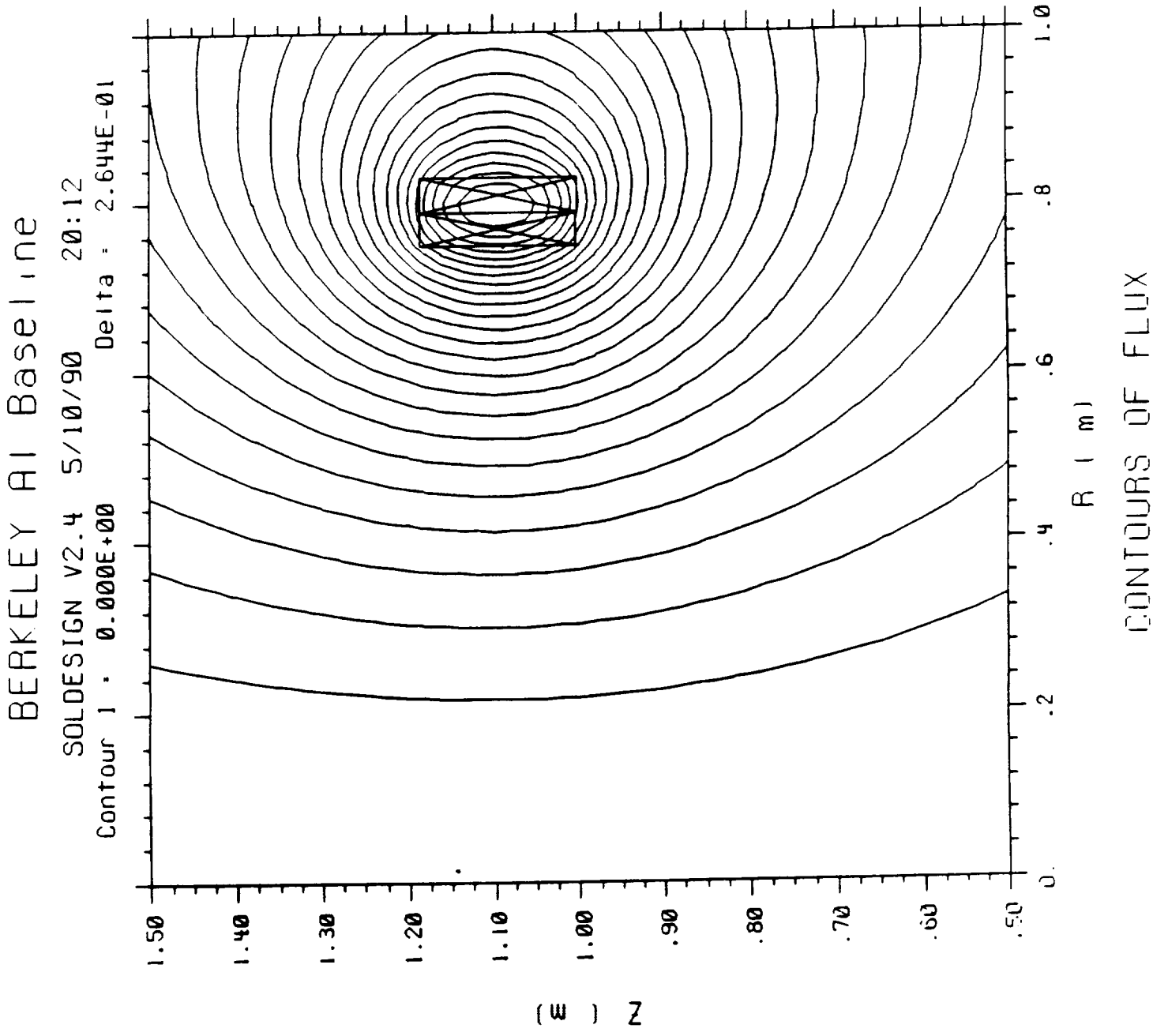

Figure 1. Baseline geometry and Flux Pattern.

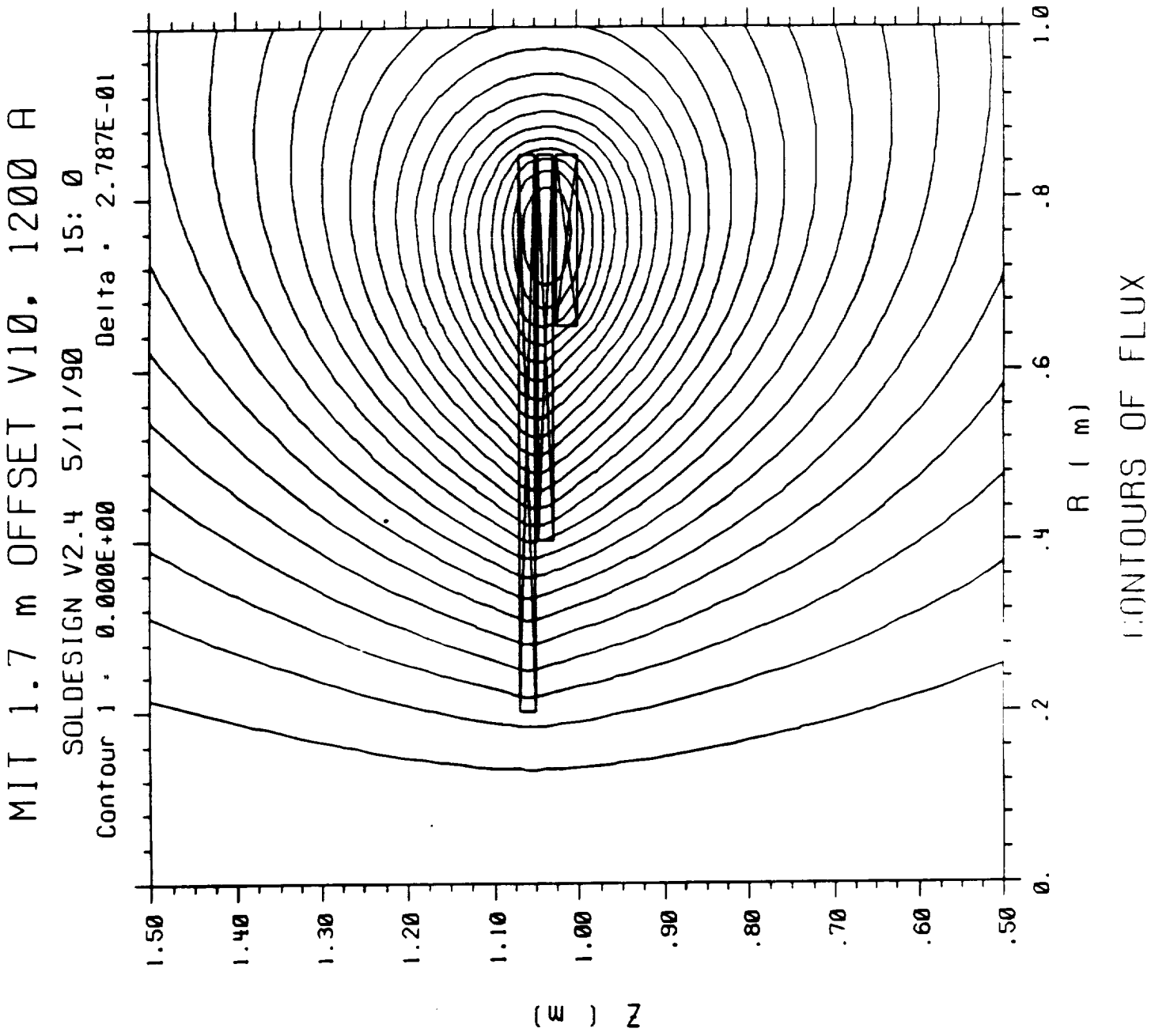

Figure 2. Disk Geometry and Flux Pattern.

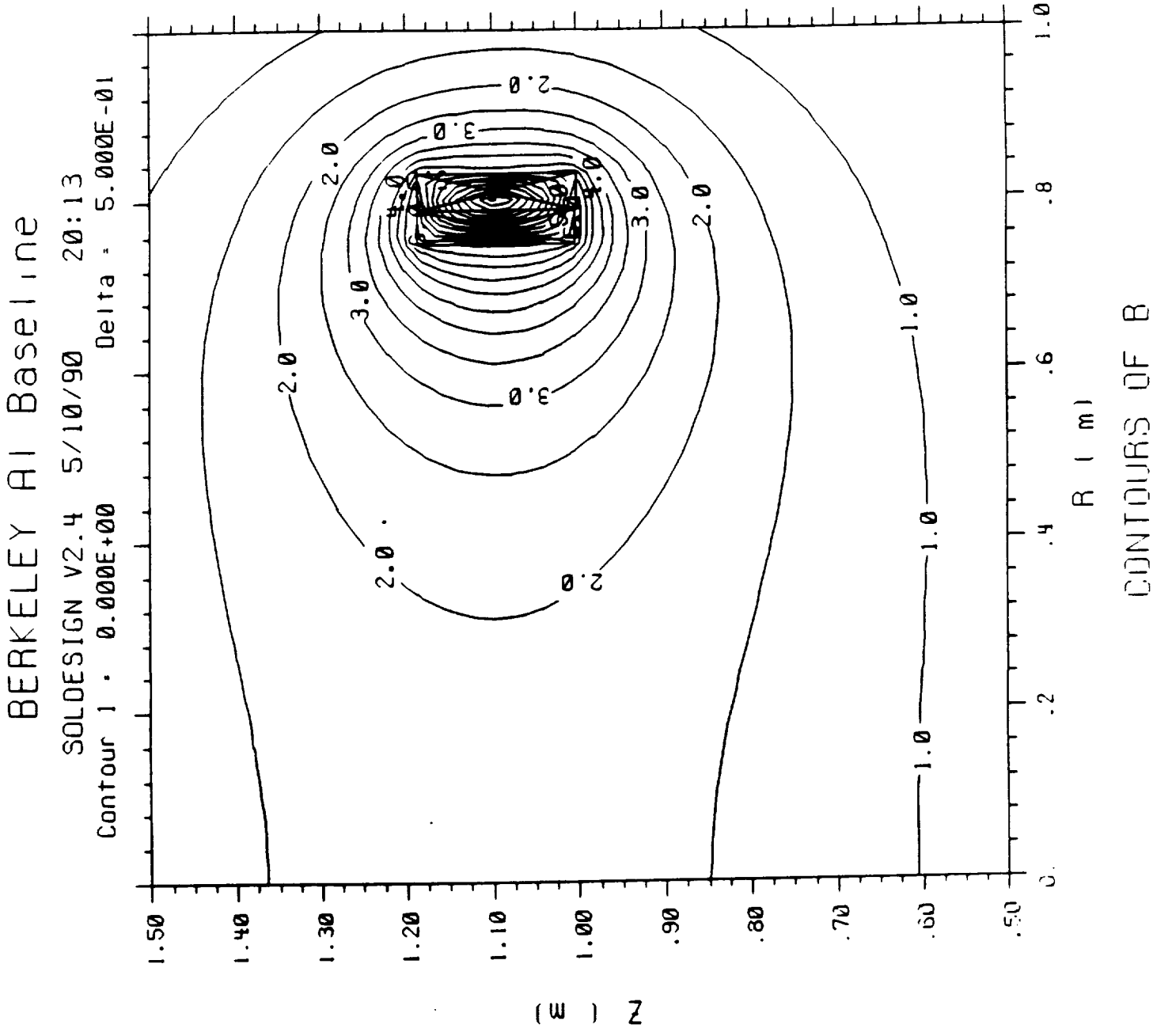

Figure 3. Baseline - Contours of Constant Flux Density (Teslas).

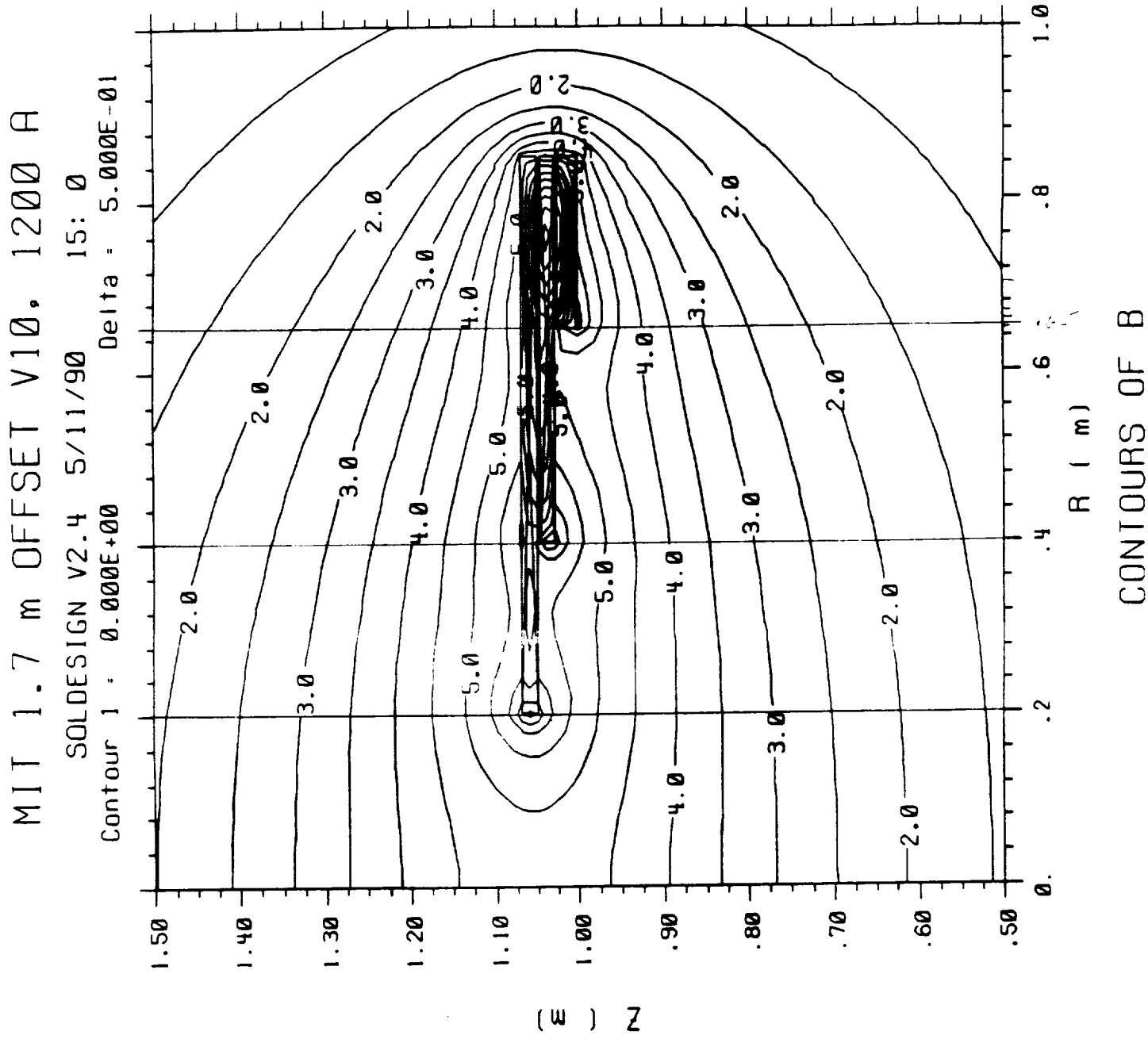

Figure 4. Disk - Contours Constant Flux Density (Teslas).

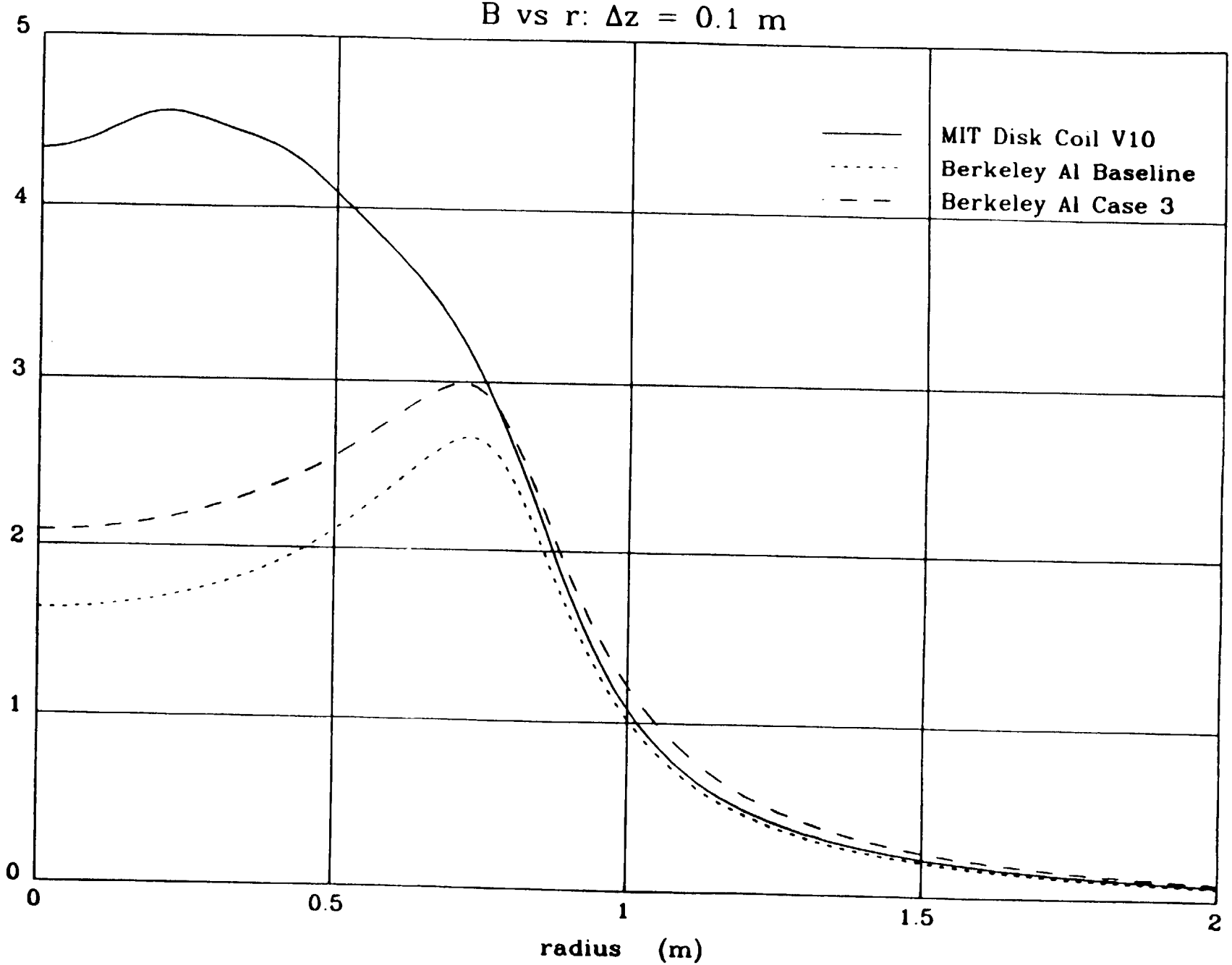
B vs r: Δz = 0.1 m
MIT Disk Coil V10
Berkeley Al Baseline
Berkeley Al Case 3
B (T)
radius (m)
0
1
2
3
4
5
0
0.5
1
1.5
2

Figure 5.

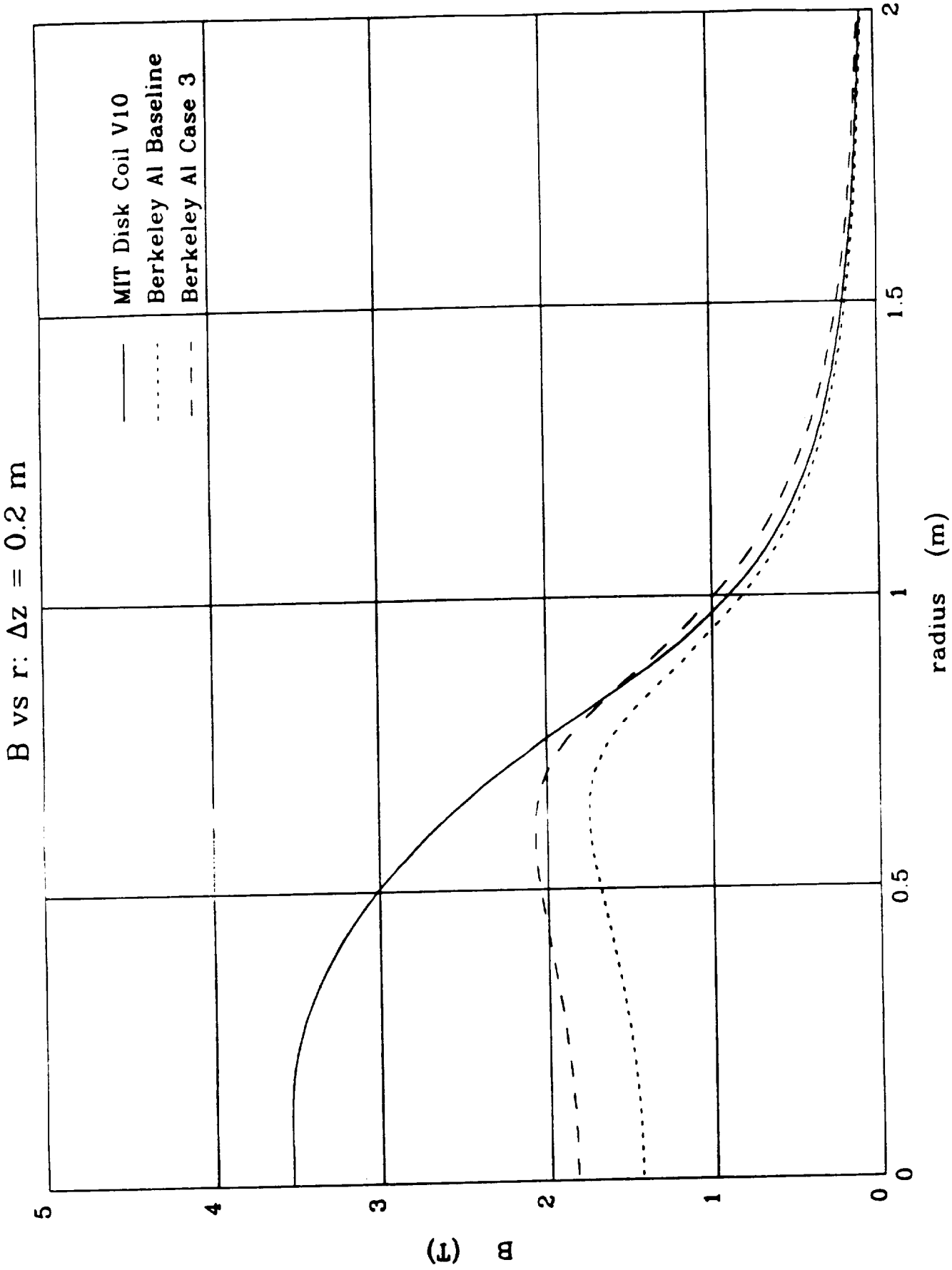
B vs r: Δz = 0.2 m
MIT Disk Coil V10
Berkeley Al Baseline
Berkeley Al Case 3
B (T)
radius (m)
0
1
2
3
4
5
0
0.5
1
1.5
2

Figure 6.

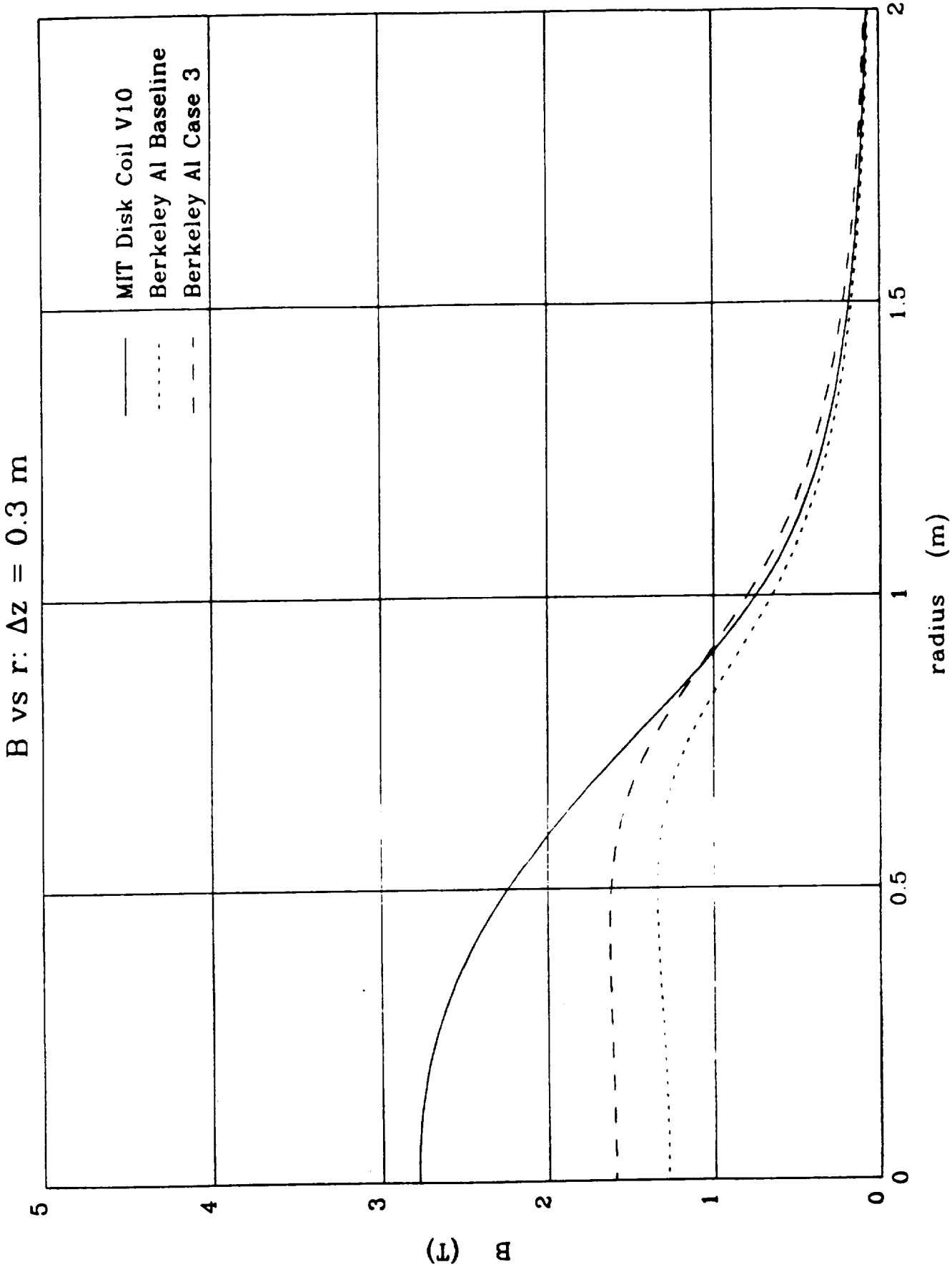
B vs r: Δz = 0.3 m
MIT Disk Coil V10
Berkeley Al Baseline
Berkeley Al Case 3
B (T)
radius (m)
0
1
2
3
4
5
0
0.5
1
1.5
2

Figure 7.

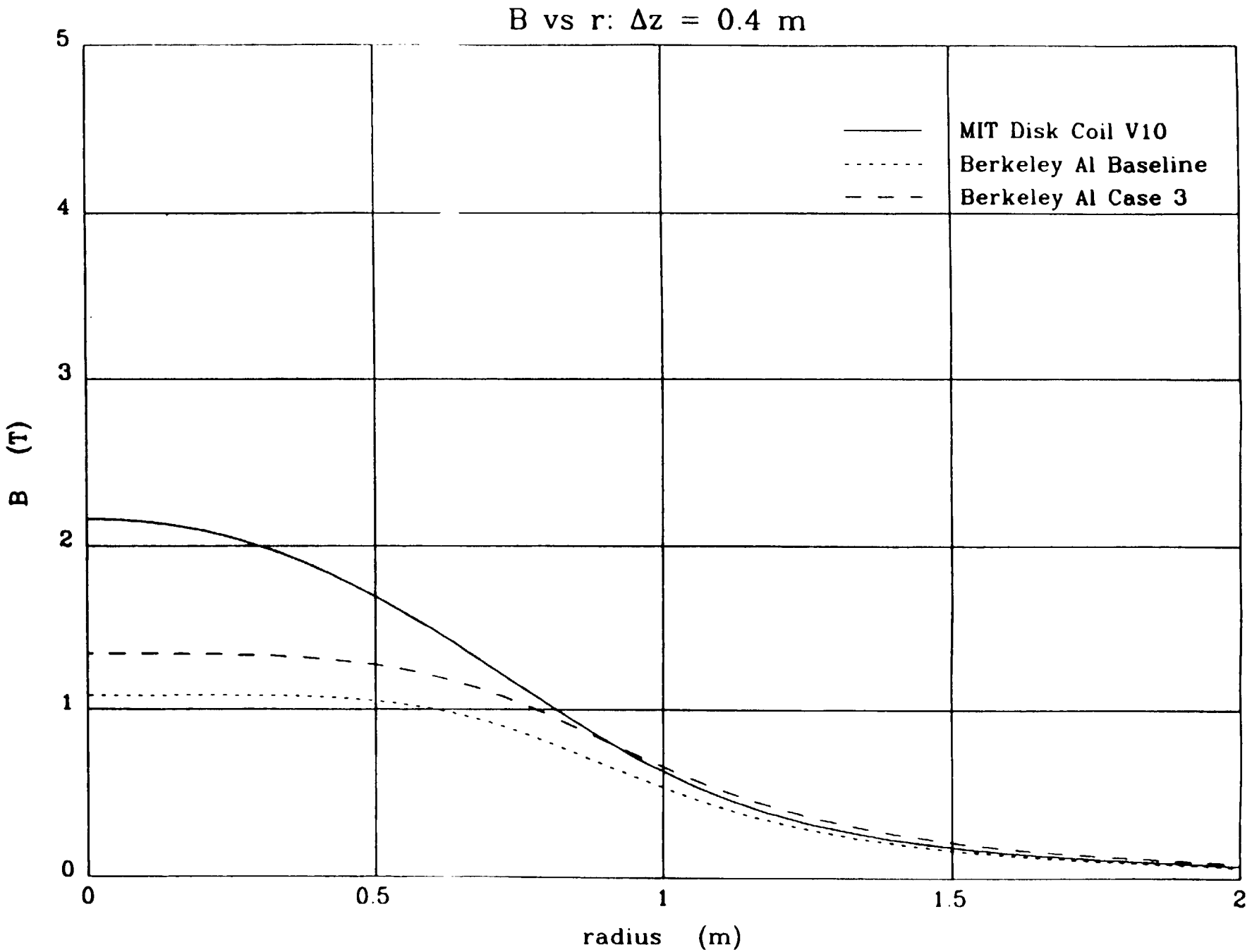
B vs r: Δz = 0.4 m
MIT Disk Coil V10
Berkeley Al Baseline
Berkeley Al Case 3
B (T)
radius (m)
0
1
2
3
4
5
0
0.5
1
1.5
2

Figure 8.

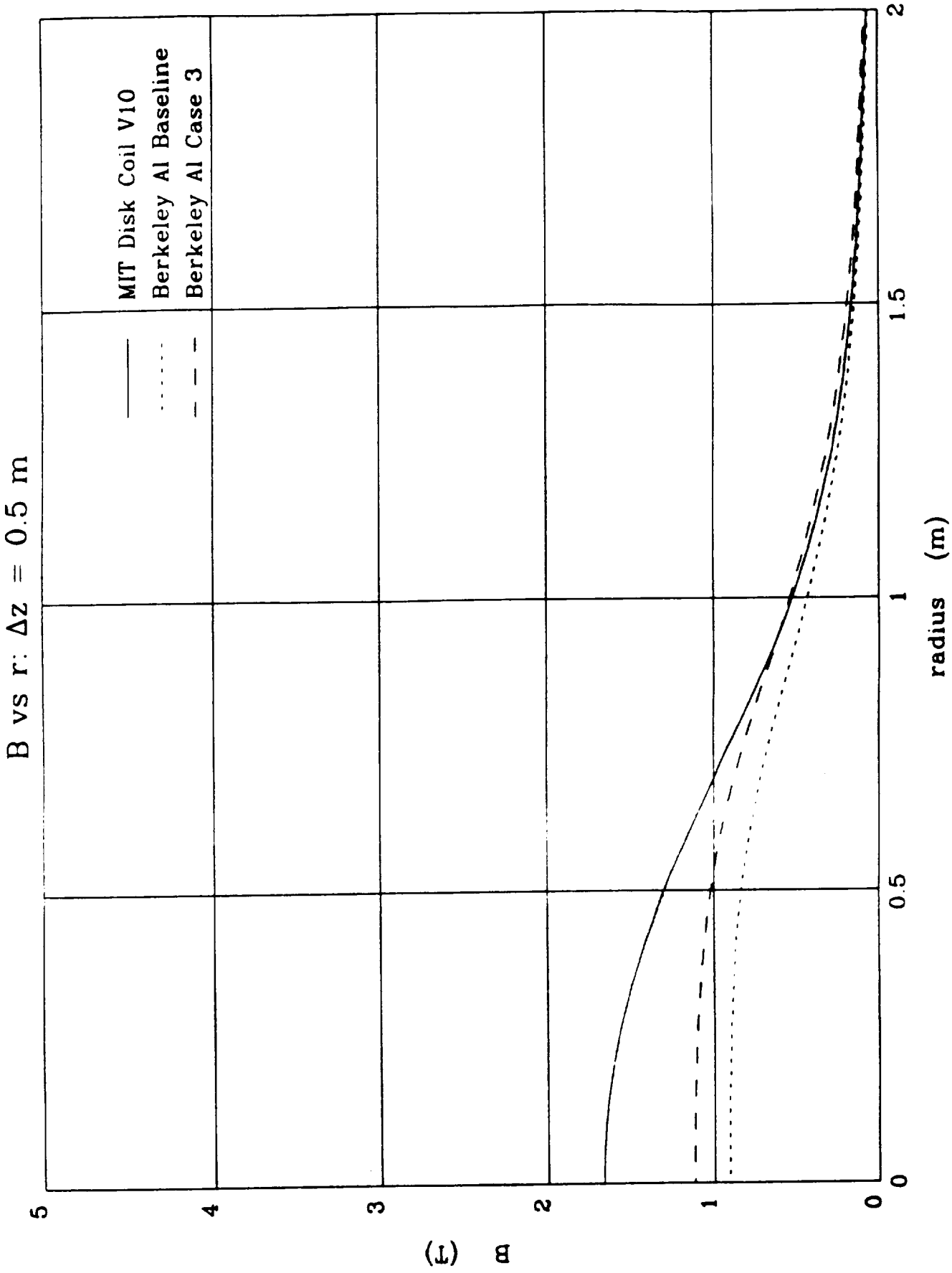
B vs r: Δz = 0.5 m
MIT Disk Coil V10
Berkeley Al Baseline
Berkeley Al Case 3
B (T)
radius (m)
0
1
2
3
4
5
0
0.5
1
1.5
2

Figure 9.

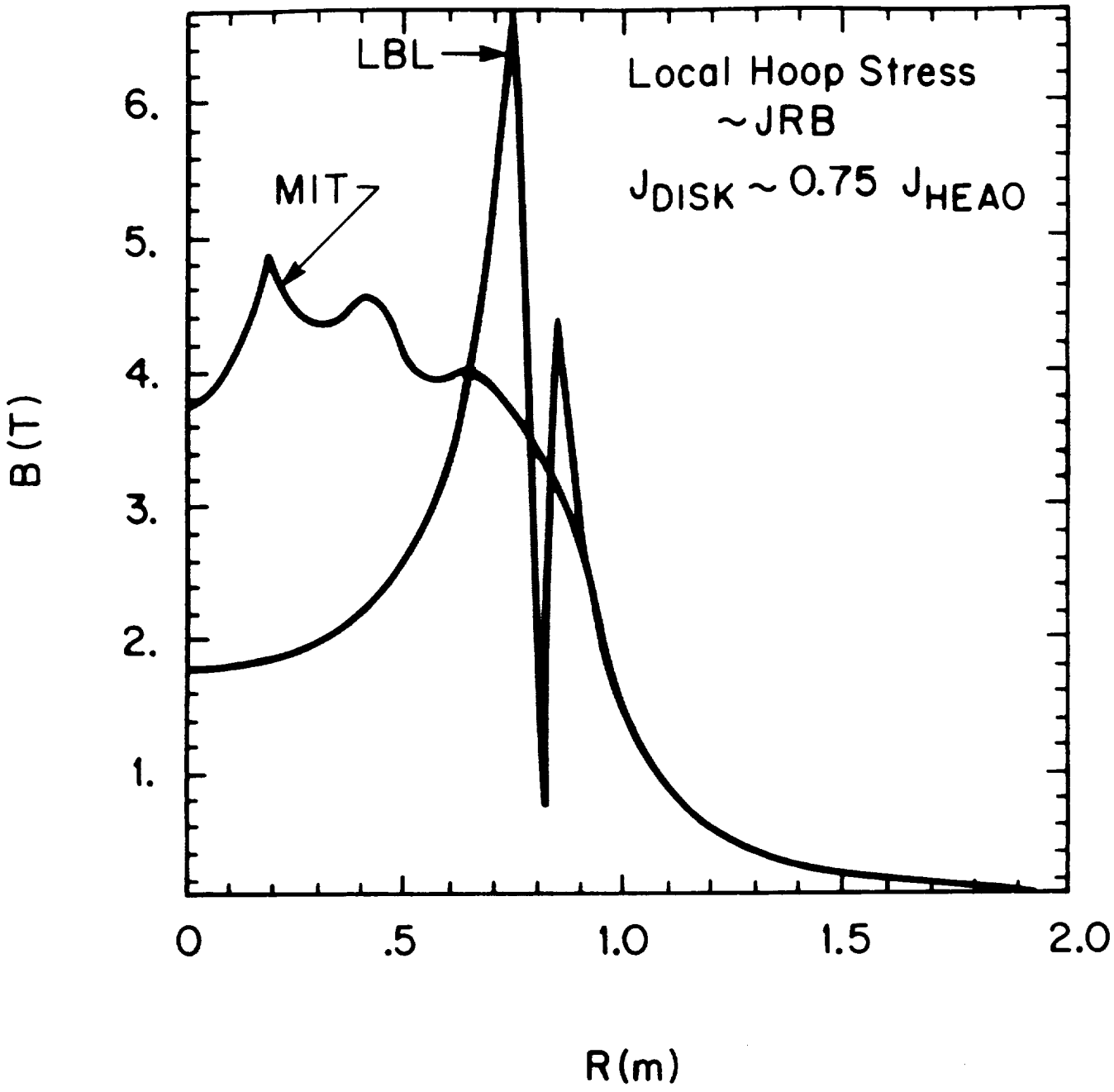

Figure 10. Peak field in the windings at 13.8 MJ

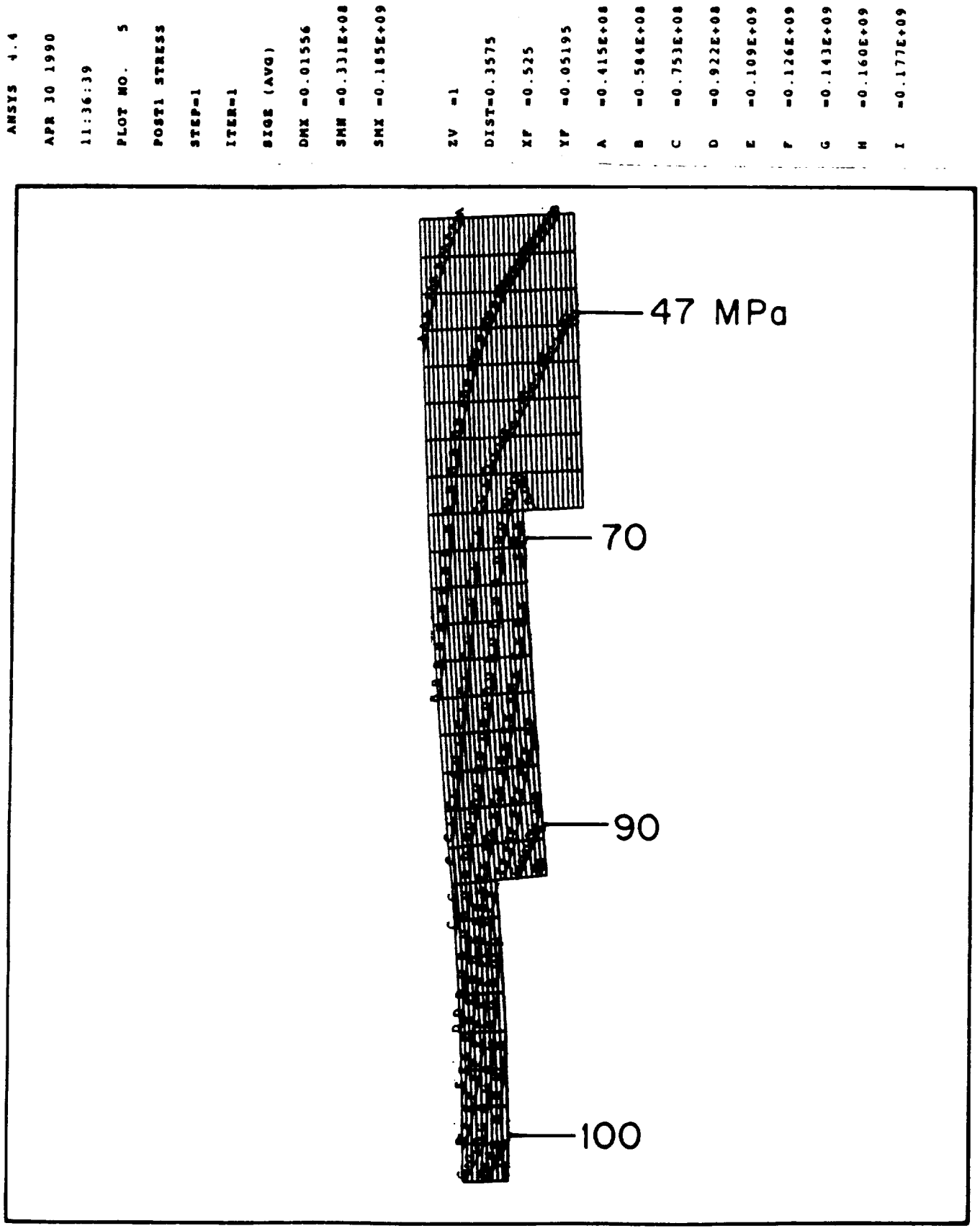

Figure 11. Disk stress distribution @ 13.8 MJ

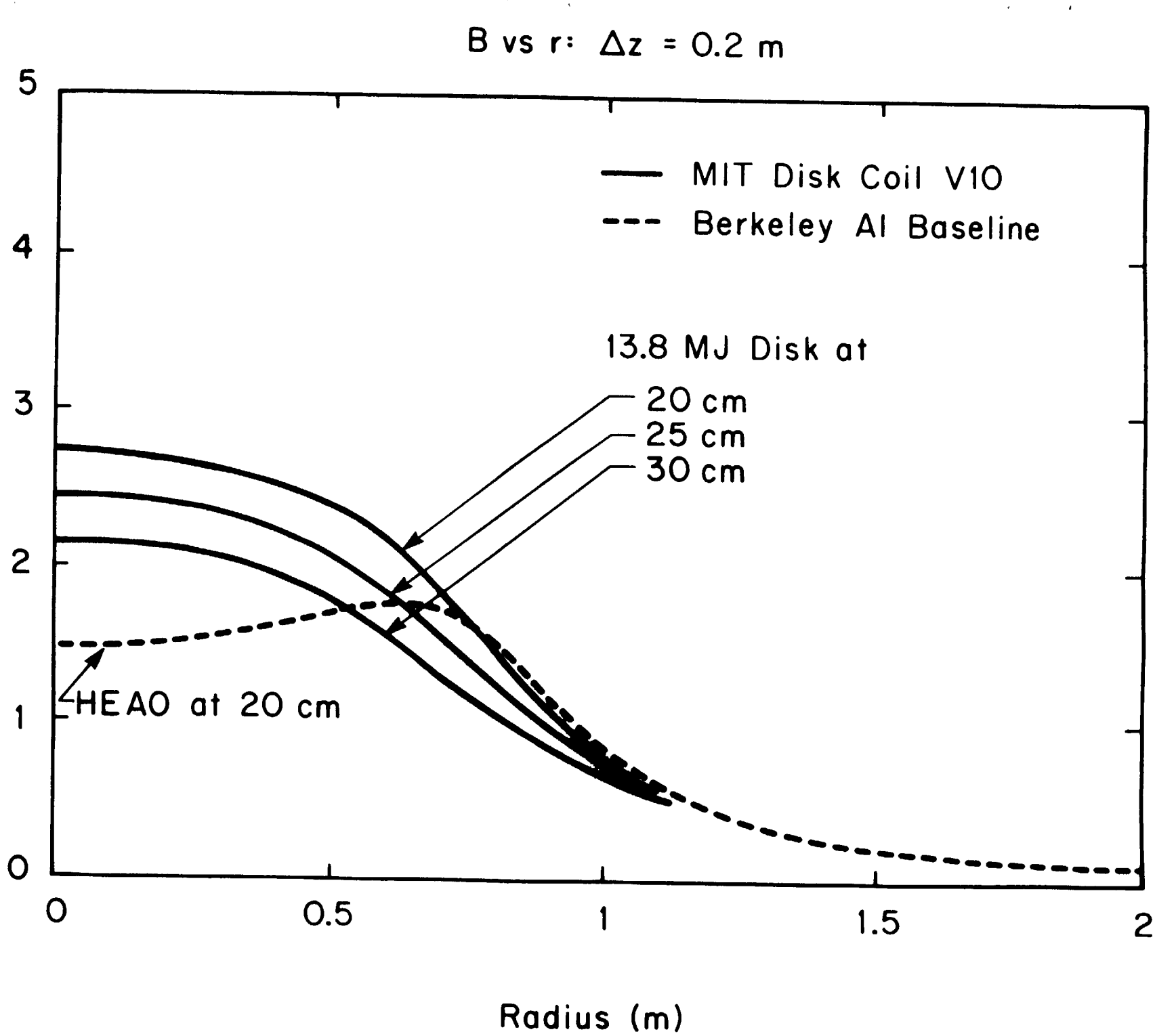
B vs r: Δz = 0.2 m
MIT Disk Coil V10
Berkeley Al Baseline
13.8 MJ Disk at
20 cm
25 cm
30 cm
HEAO at 20 cm
B (T)
Radius (m)
0
1
2
3
4
5
0
0.5
1
1.5
2

Figure 12
24

APPENDIX A

Design of an Opposing Pair Magnet System for ASTROMAG.

Presented at the 1990 Applied Superconducvitity Conference, Snowmass, Co., September 1990.

APPENDIX B

FIELD PLOTS FOR DESIGNS V10, V18 AND R5

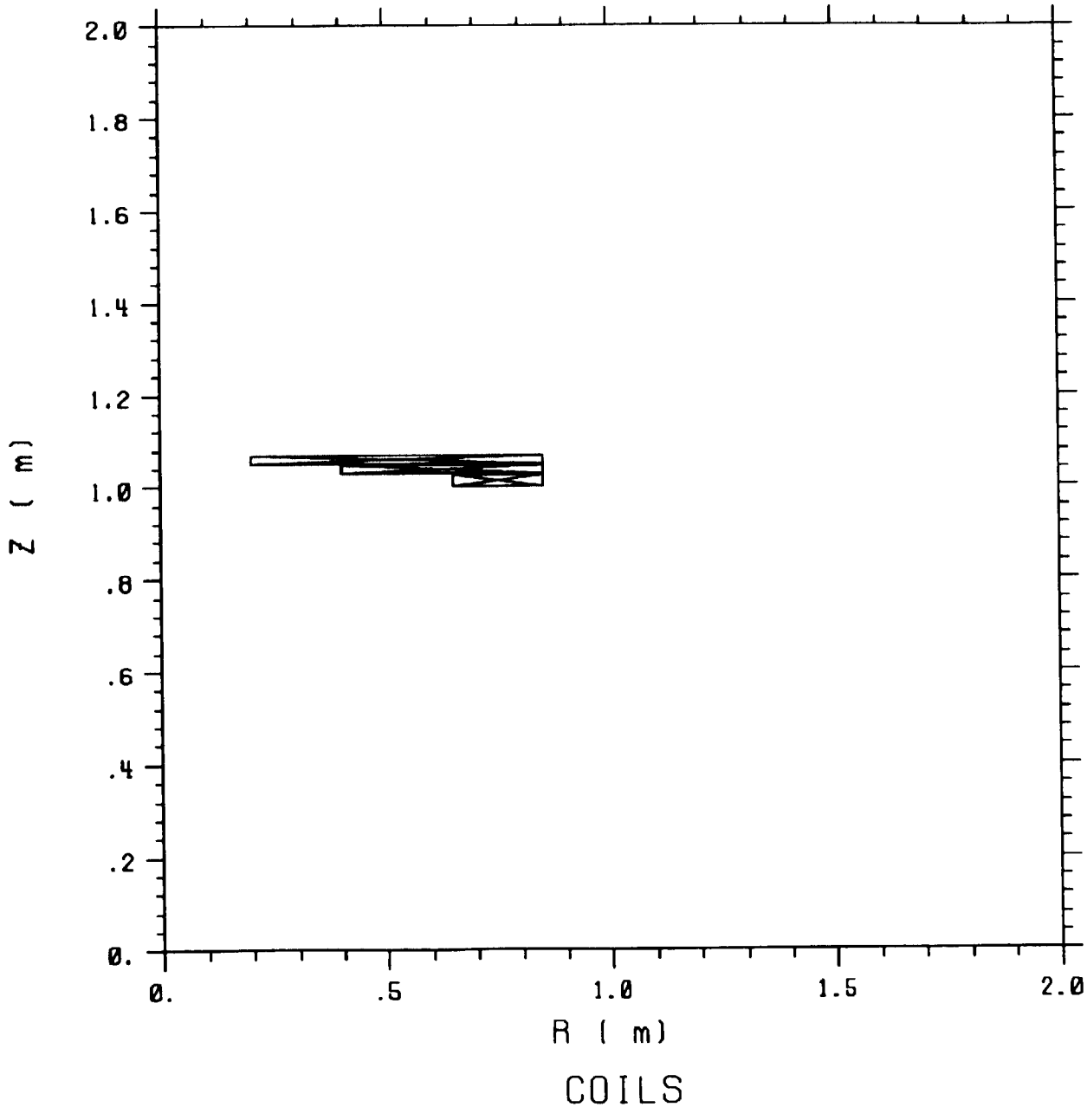
MIT 1.7 m OFFSET V10, 1200 A
SOLDESIGN V2.4 7/17/90 14:29
2.0
1.8
1.6
1.4
1.2
1.0
.8
.6
.4
.2
0.
Z (m)
0.
.5
1.0
1.5
2.0
R (m)
COILS

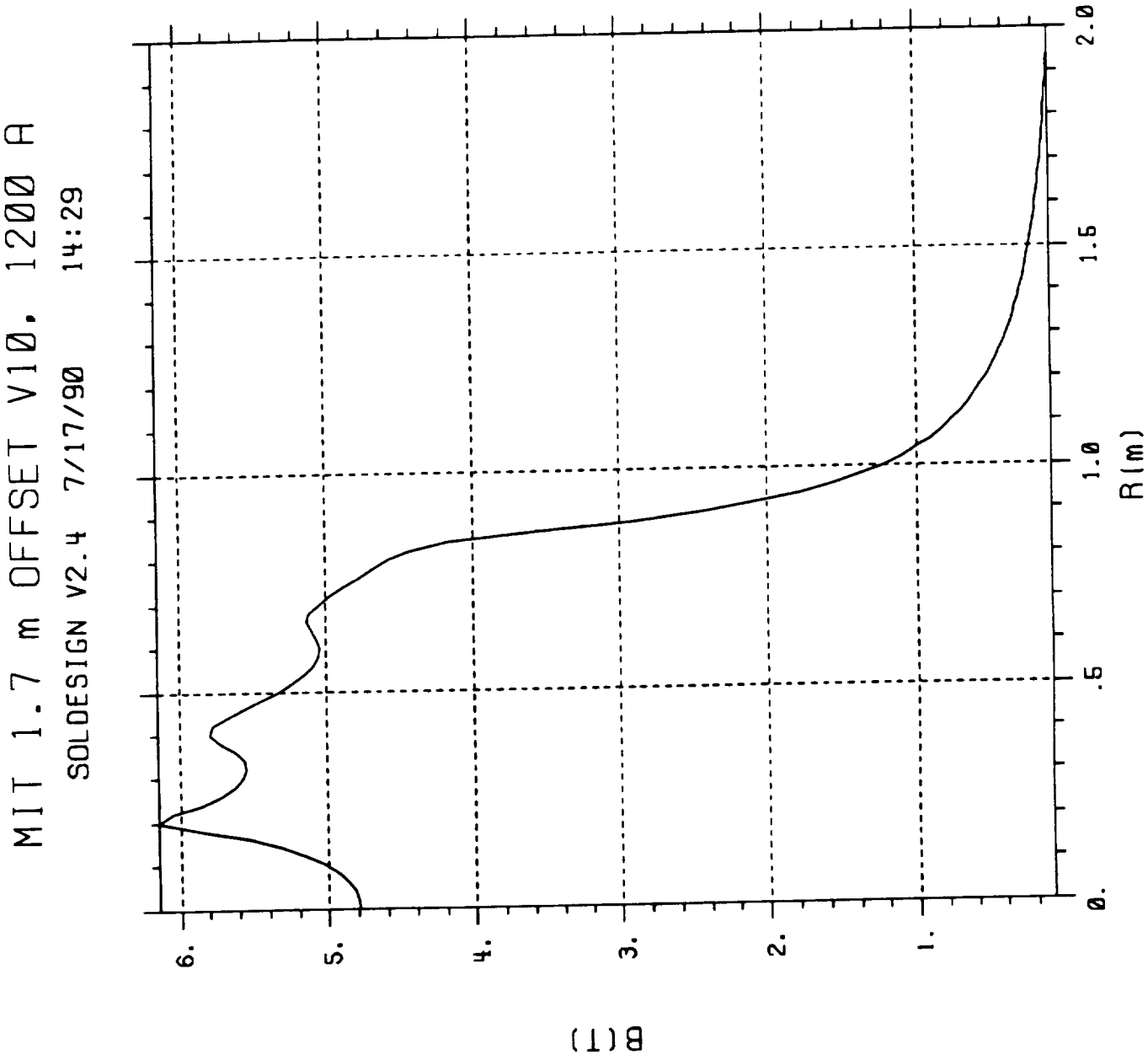

B vs R @ Z = 1.08 m showing B_{max} at I.D.

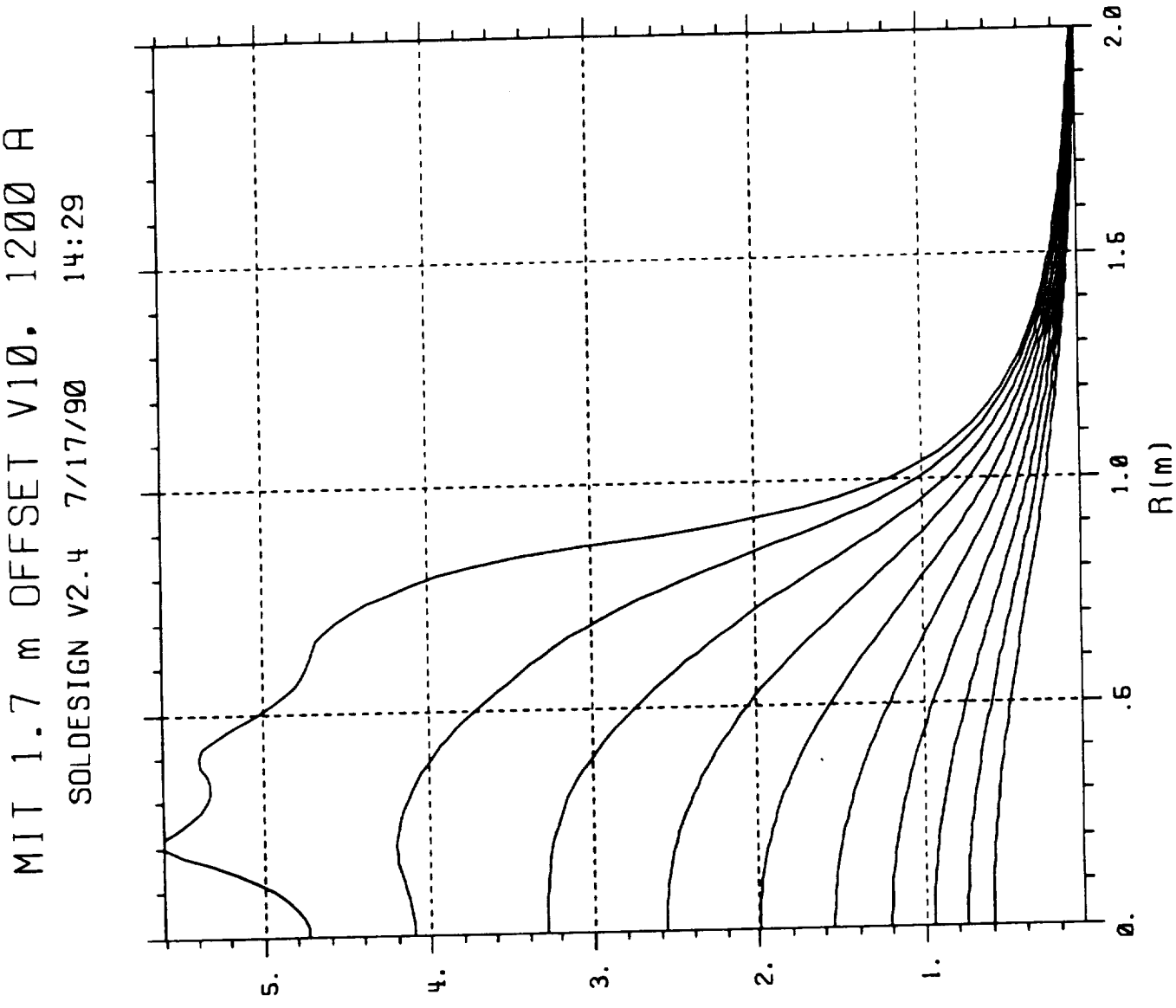

B vs R, with ΔZ = 10 cm. First (uppermost) curve @ Z = 1.10 m

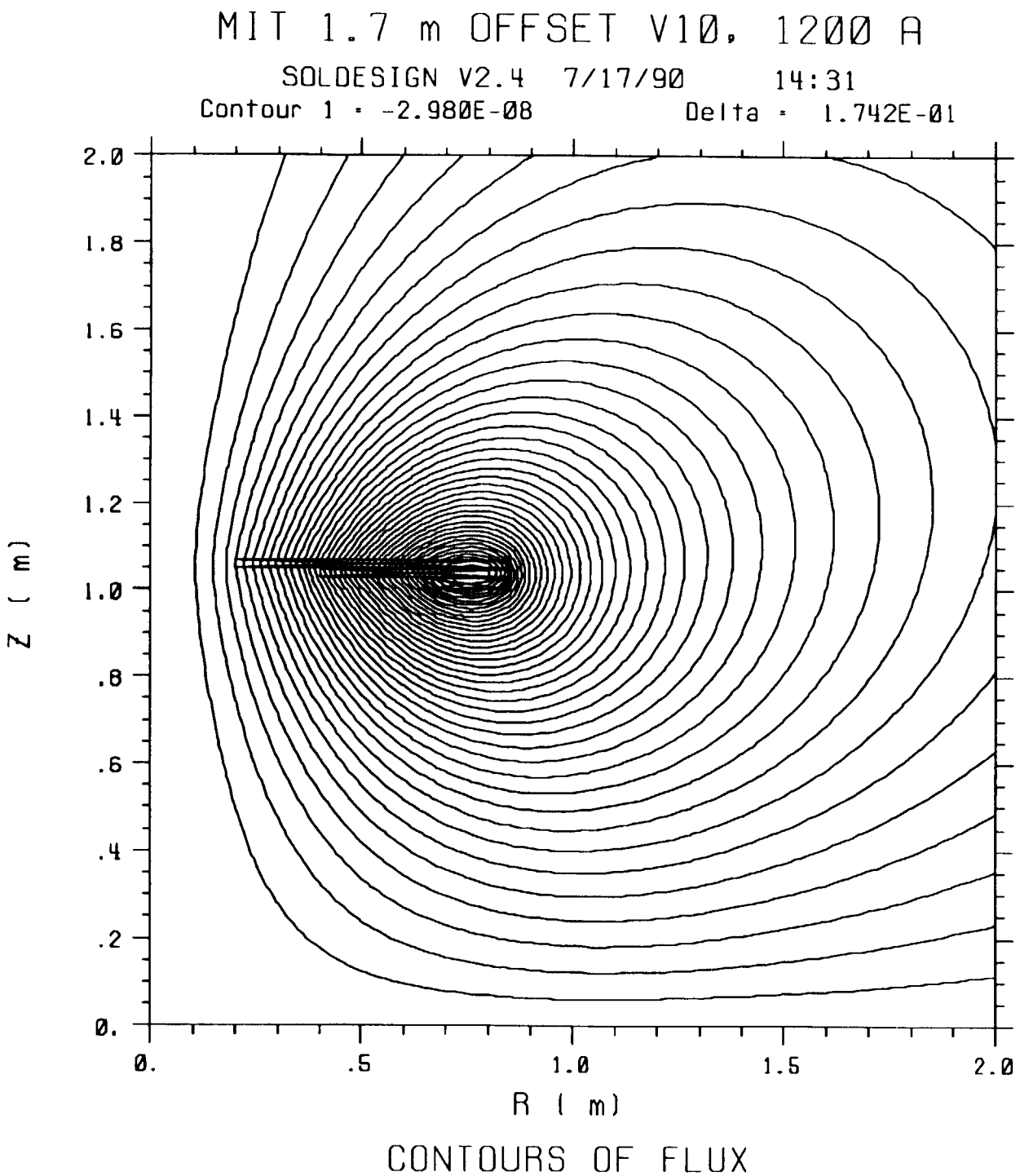
MIT 1.7 m OFFSET V10, 1200 A
SOLDESIGN V2.4 7/17/90 14:31
Contour 1 = -2.980E-08 Delta = 1.742E-01
2.0
1.8
1.6
1.4
1.2
1.0
.8
.6
.4
.2
0.
Z (m)
0.
.5
1.0
1.5
2.0
R (m)
CONTOURS OF FLUX

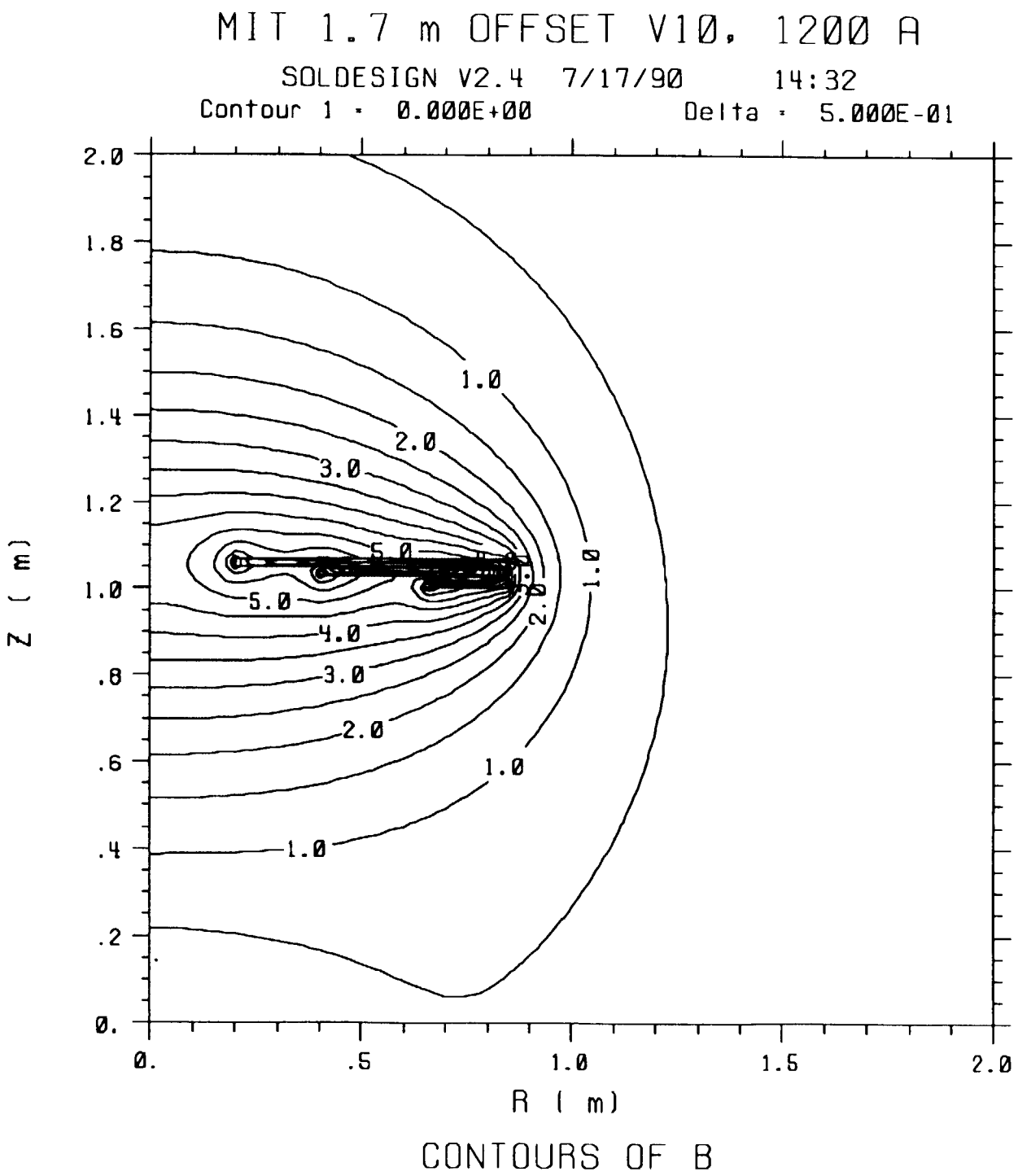
MIT 1.7 m OFFSET V10, 1200 A
SOLDESIGN V2.4 7/17/90 14:32
Contour 1 = 0.000E+00 Delta = 5.000E-01
2.0
1.8
1.6
1.4
1.2
1.0
.8
.6
.4
.2
0.
Z (m)
0.
.5
1.0
1.5
2.0
R (m)
1.0
2.0
3.0
5.0
4.0
CONTOURS OF B

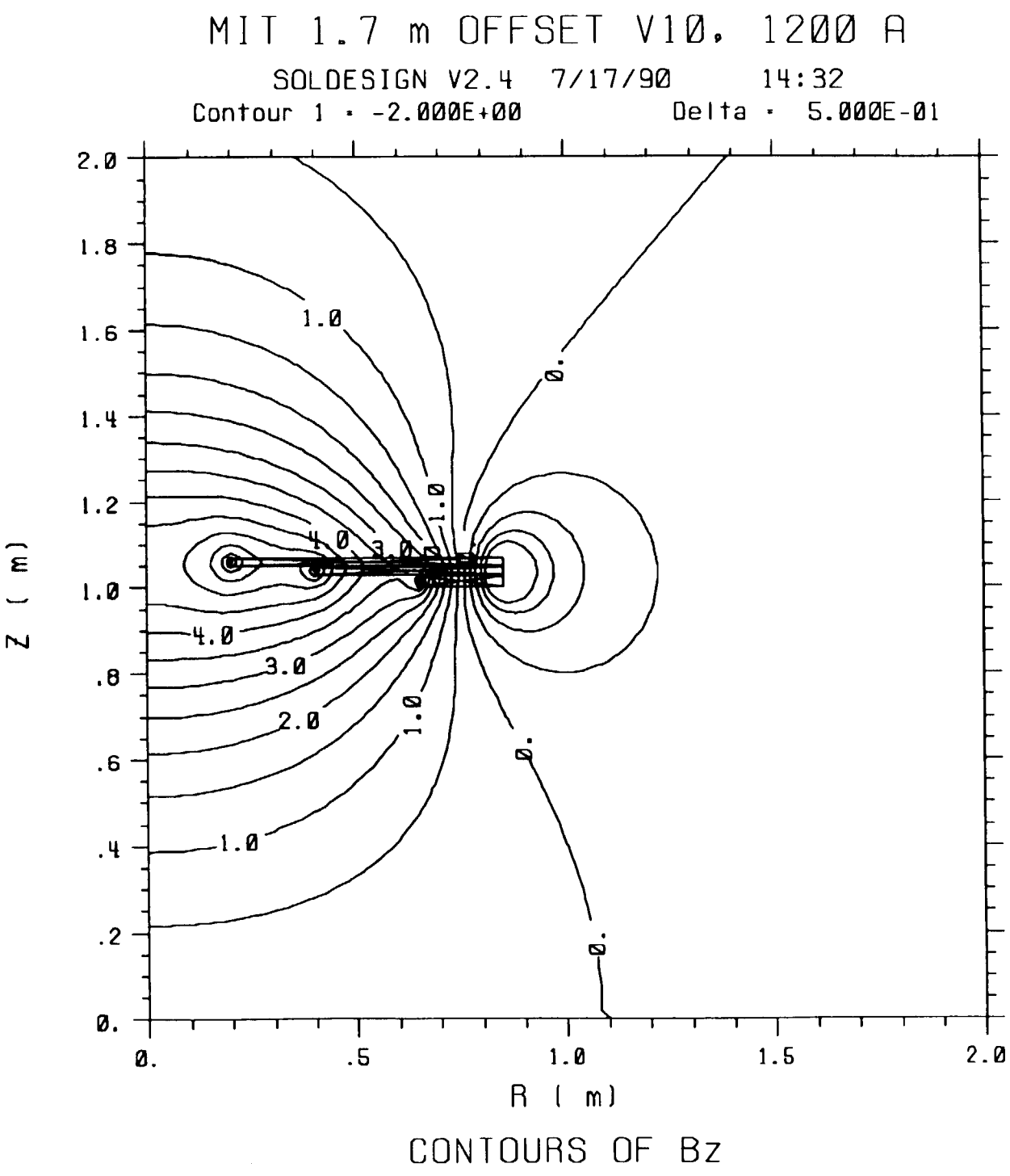
MIT 1.7 m OFFSET V10, 1200 A
SOLDESIGN V2.4 7/17/90 14:32
Contour 1 = -2.000E+00 Delta = 5.000E-01
2.0
1.8
1.6
1.4
1.2
1.0
.8
.6
.4
.2
0.
Z (m)
1.0
0.
1.0
4.0
3.0
4.0
3.0
2.0
1.0
1.0
0.
0.
0.
.5
1.0
1.5
2.0
R (m)
CONTOURS OF Bz

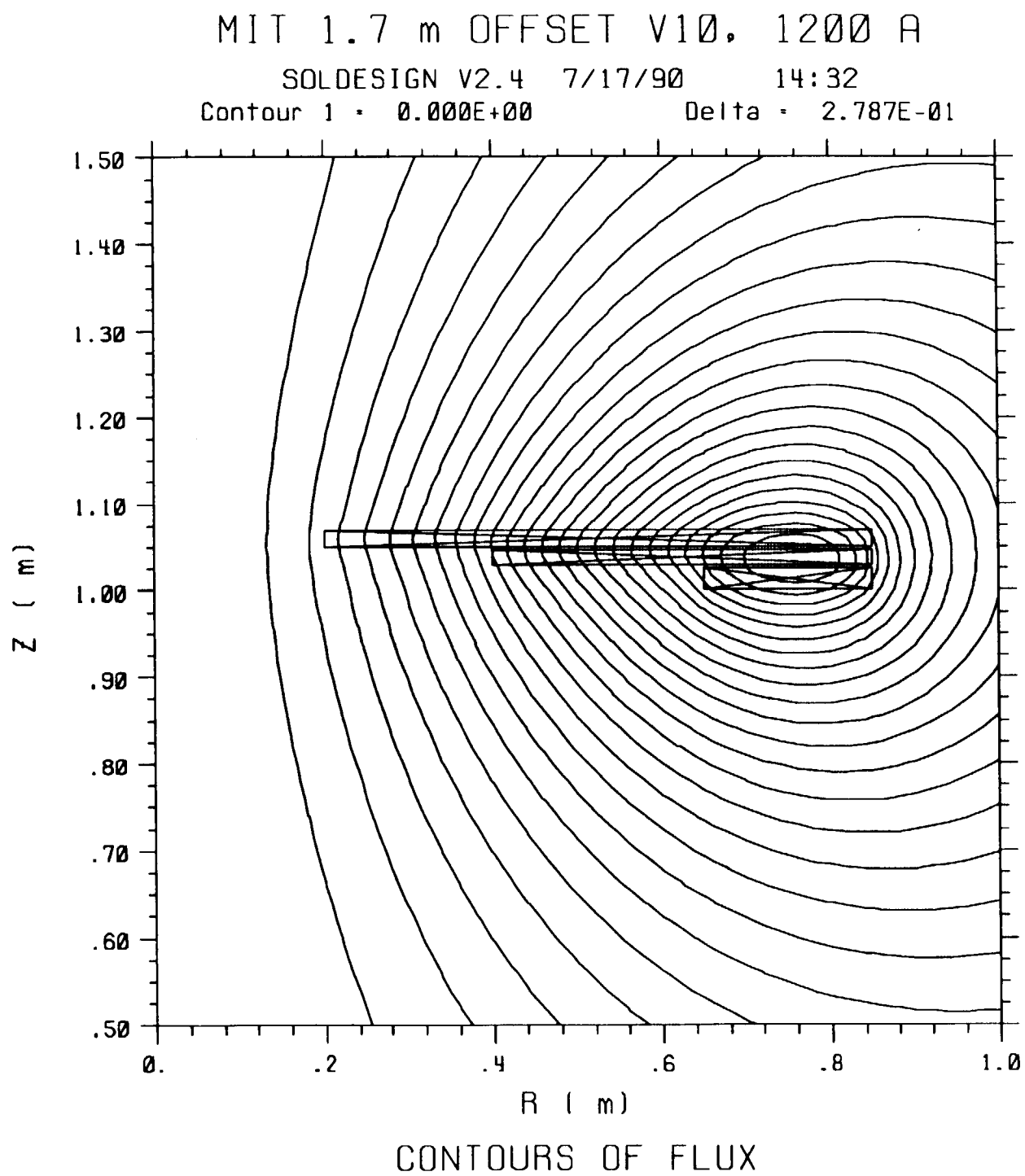

CONTOURS OF FLUX

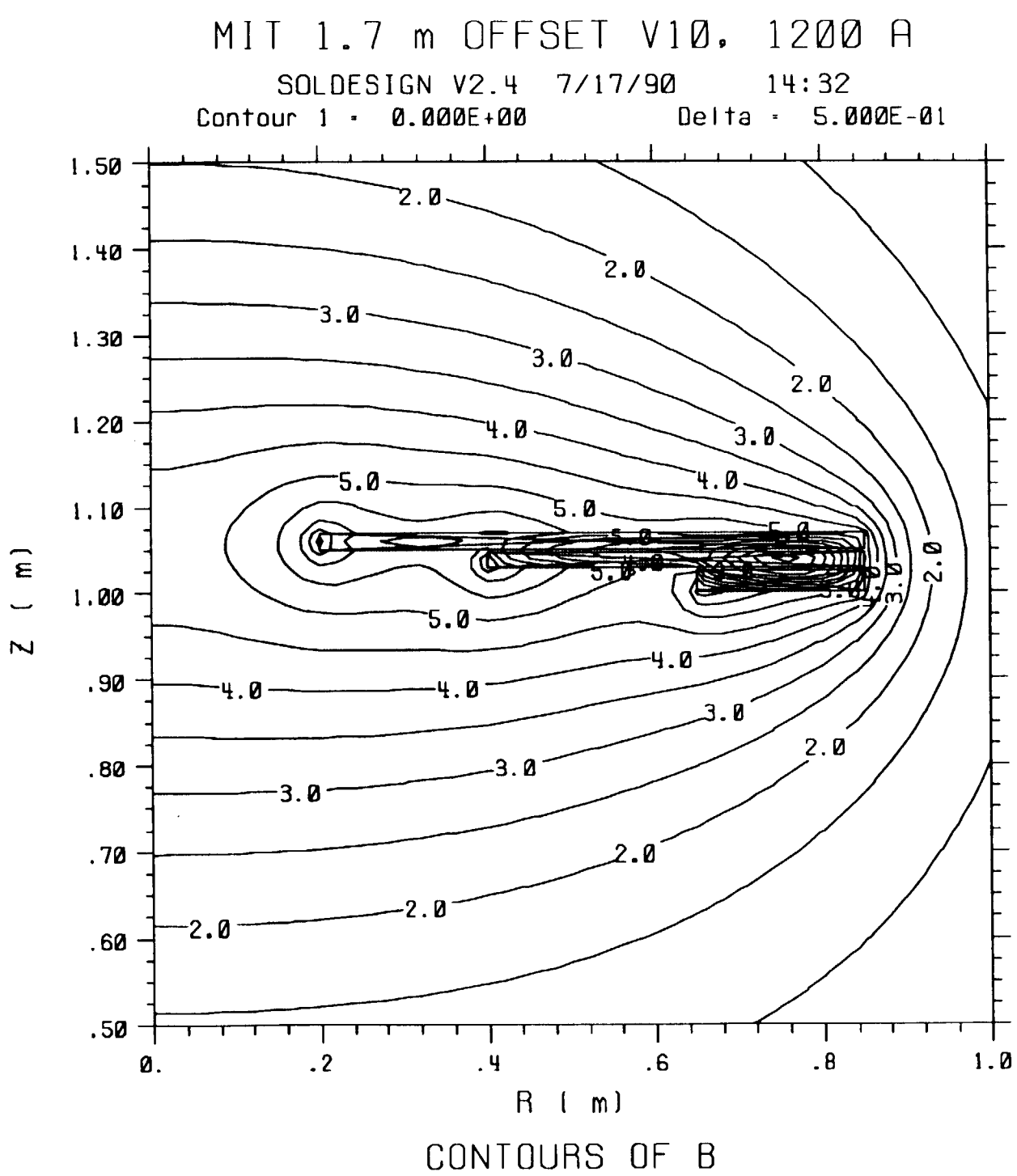

CONTOURS OF B

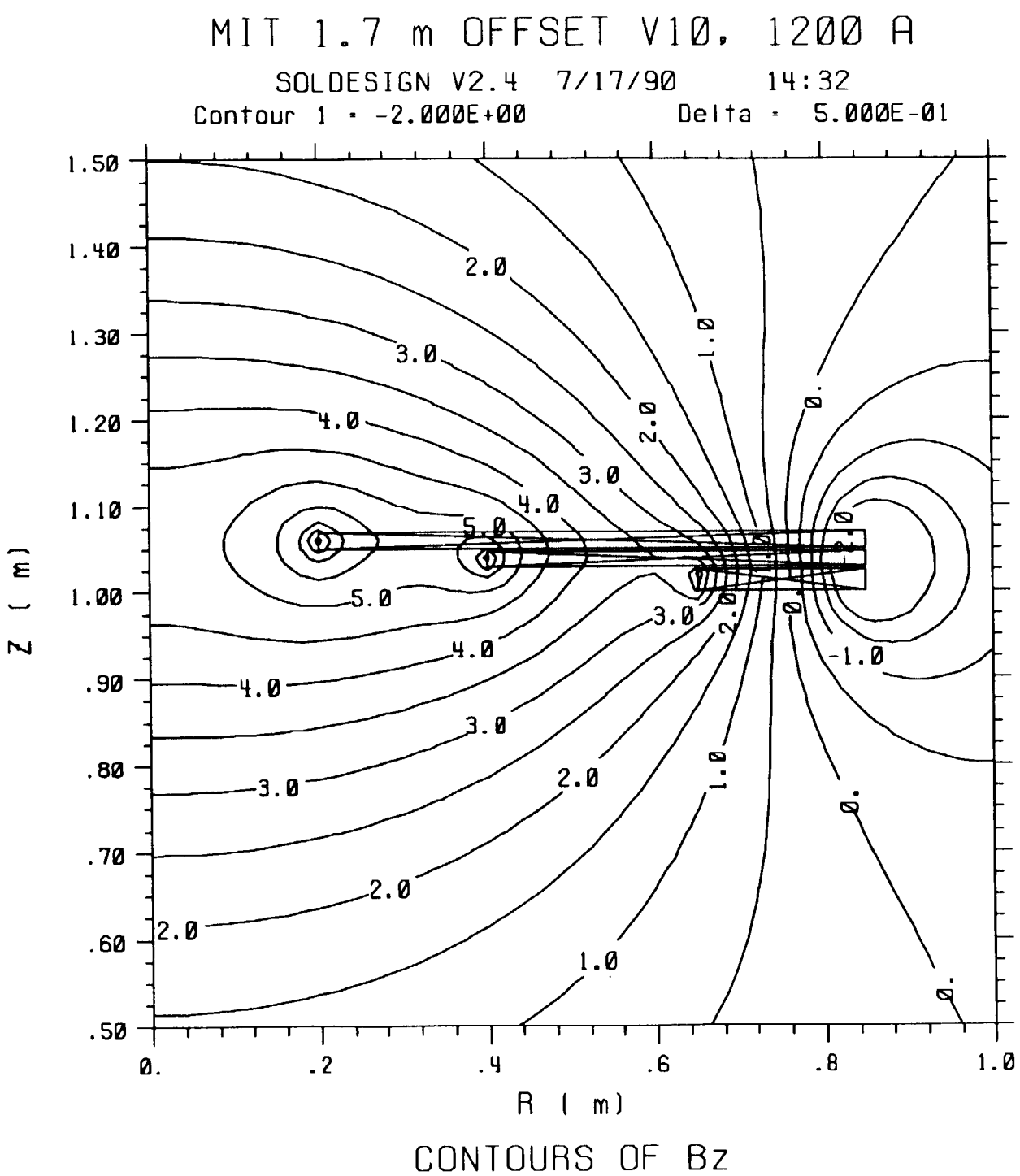

CONTOURS OF Bz

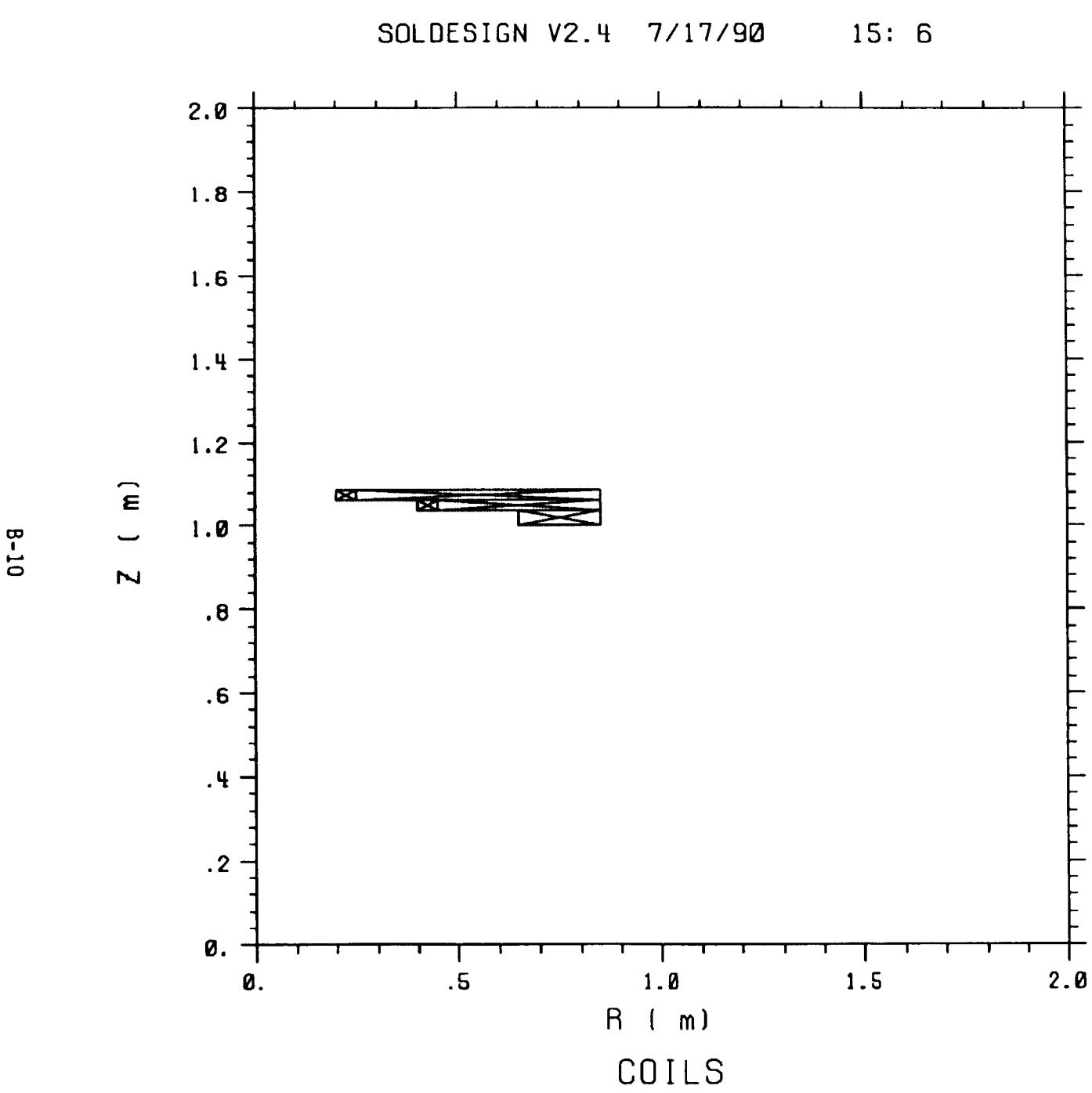
MIT 1.7 m OFFSET V18, 1000 A
SOLDESIGN V2.4 7/17/90 15: 6
2.0
1.8
1.6
1.4
1.2
1.0
.8
.6
.4
.2
0.
Z (m)
0.
.5
1.0
1.5
2.0
R (m)
COILS

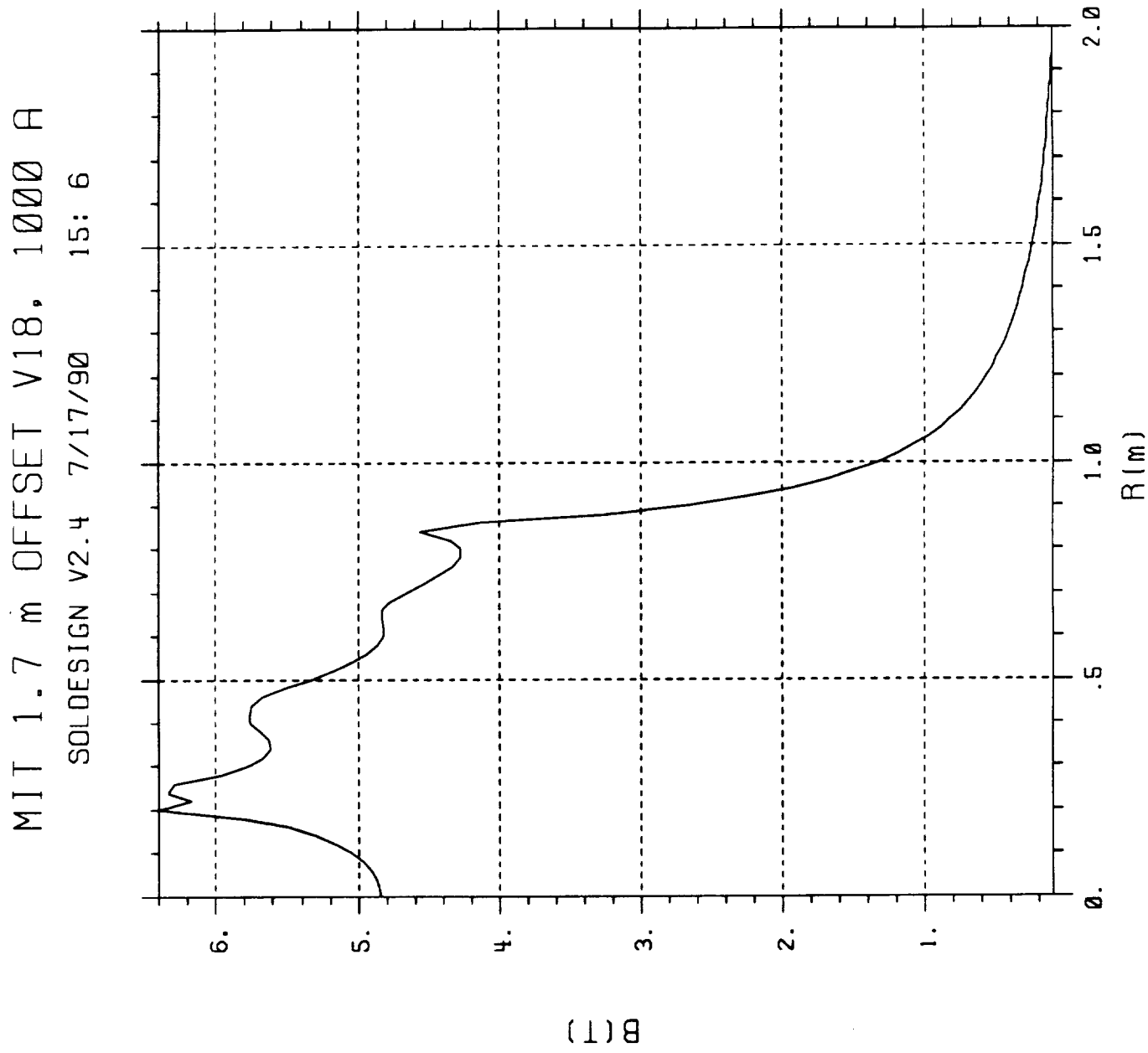

B vs R @ Z = 1.08 m showing B_{max} at ID.

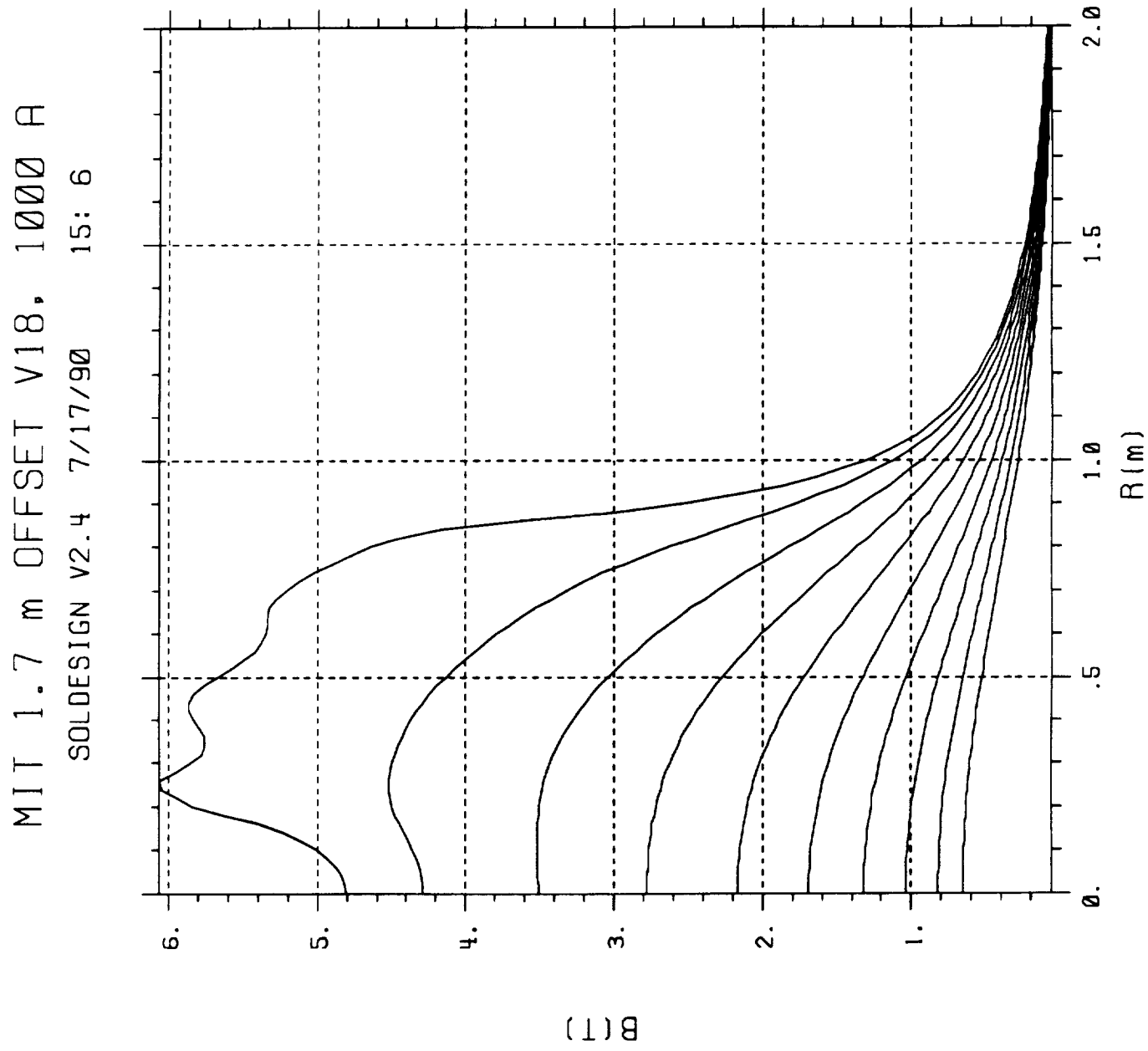

B vs R, ΔZ = 10 cm. First (uppermost) curve at Z = 1.1 m.

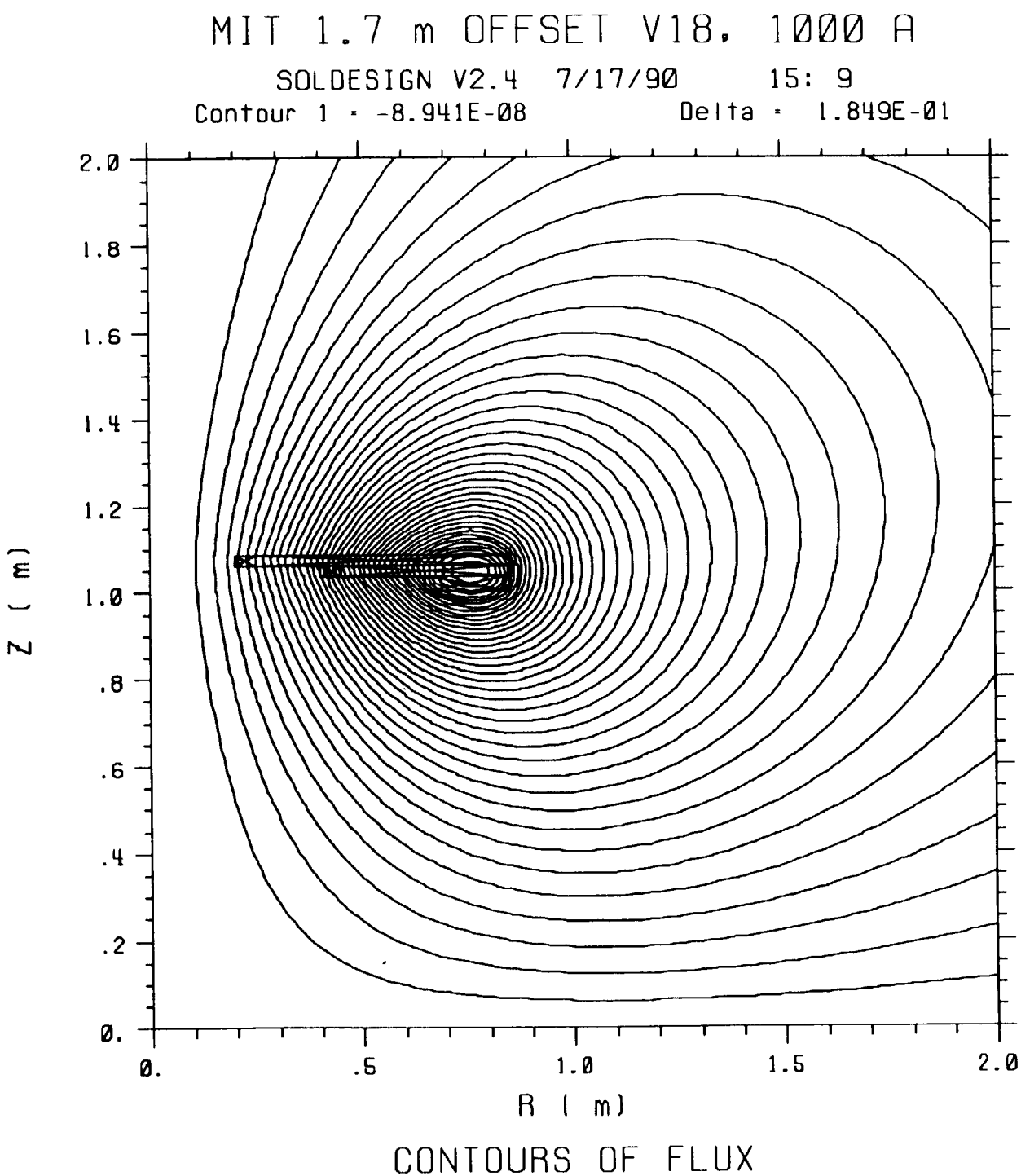
MIT 1.7 m OFFSET V18, 1000 A
SOLDESIGN V2.4 7/17/90 15: 9
Contour 1 = -8.941E-08 Delta = 1.849E-01
2.0
1.8
1.6
1.4
1.2
1.0
.8
.6
.4
.2
0.
Z (m)
0.
.5
1.0
1.5
2.0
R (m)
CONTOURS OF FLUX

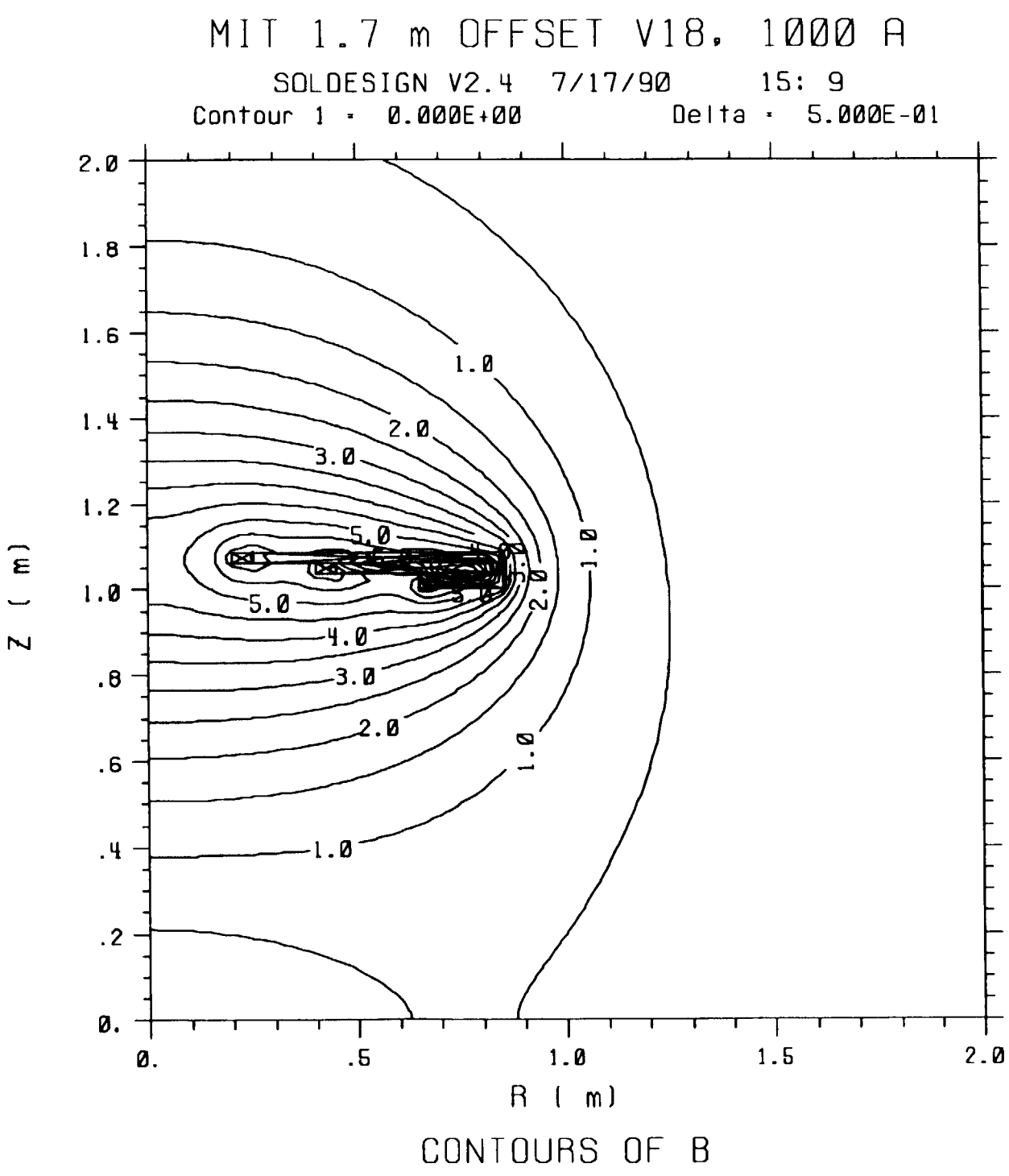
MIT 1.7 m OFFSET V18, 1000 A
SOLDESIGN V2.4 7/17/90 15: 9
Contour 1 = 0.000E+00 Delta = 5.000E-01
2.0
1.8
1.6
1.4
1.2
1.0
.8
.6
.4
.2
0.
Z (m)
0.
.5
1.0
1.5
2.0
R (m)
1.0
2.0
3.0
5.0
5.0
4.0
3.0
2.0
1.0
1.0
2.0
1.0
CONTOURS OF B

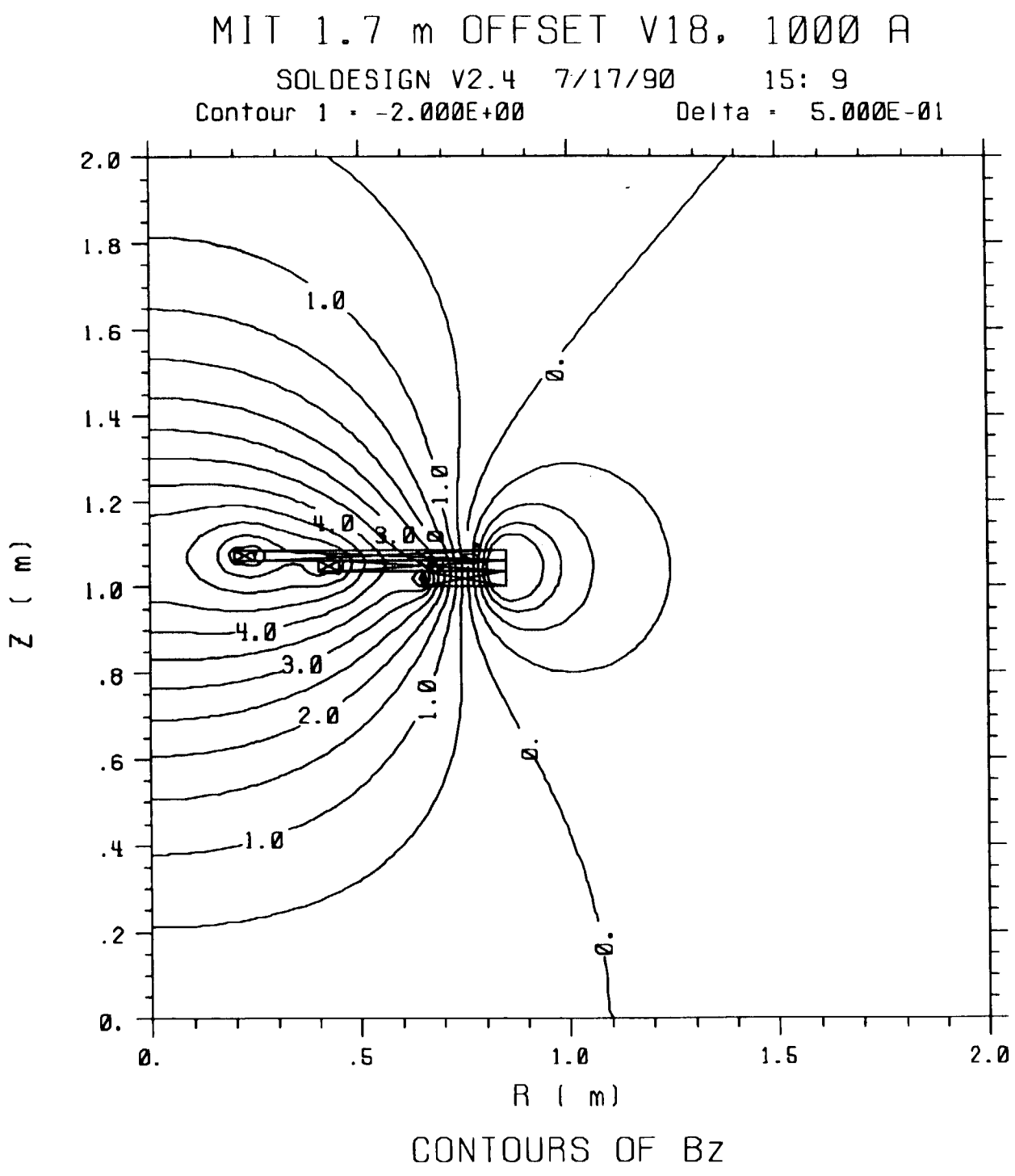
MIT 1.7 m OFFSET V18, 1000 A
SOLDESIGN V2.4 7/17/90 15: 9
Contour 1 = -2.000E+00 Delta = 5.000E-01
2.0
1.8
1.6
1.4
1.2
1.0
.8
.6
.4
.2
0.
Z (m)
1.0
0.
1.0
4.0
3.0
2.0
1.0
4.0
3.0
2.0
1.0
0.
0.
0.
.5
1.0
1.5
2.0
R (m)
CONTOURS OF Bz

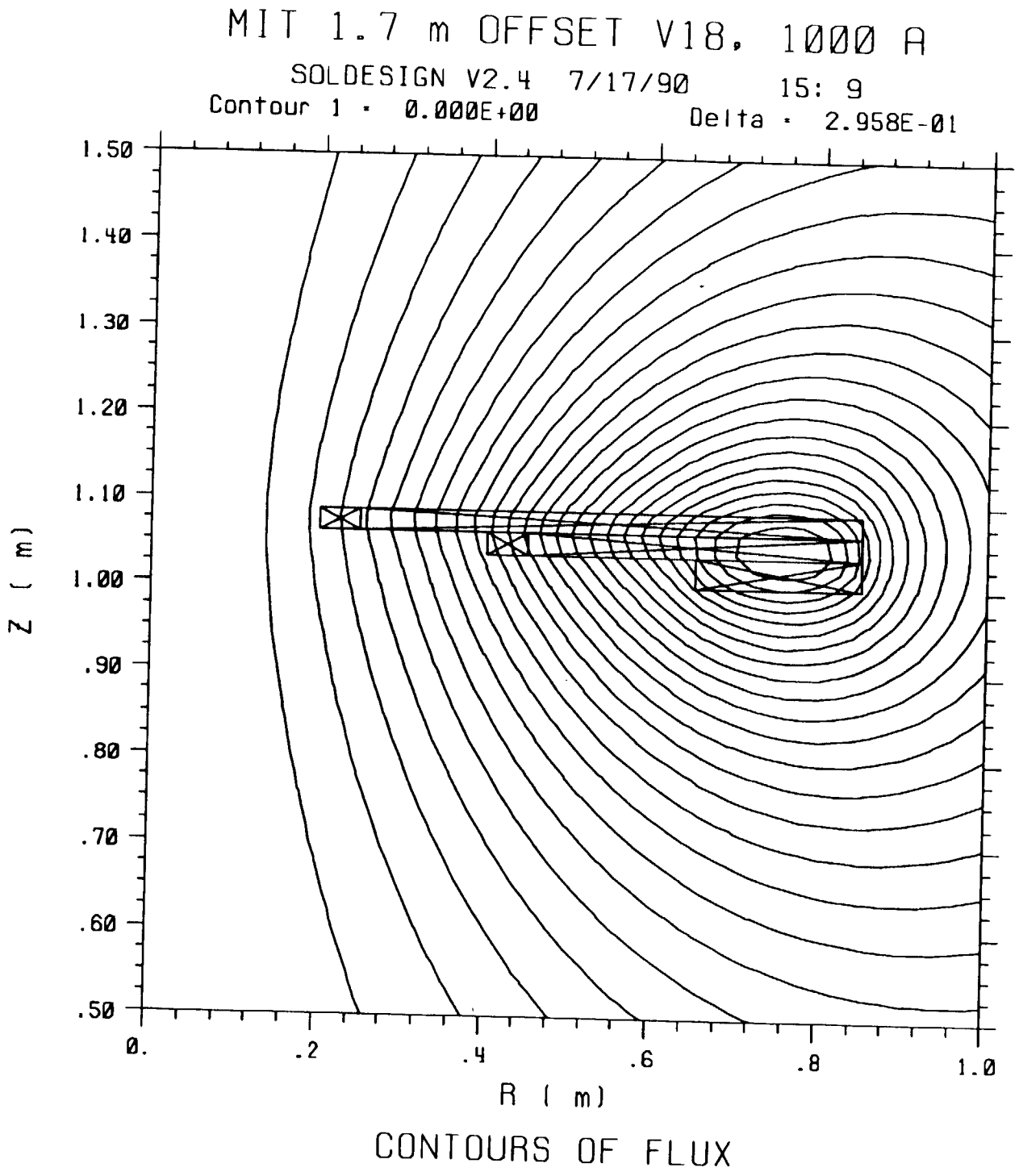

CONTOURS OF FLUX

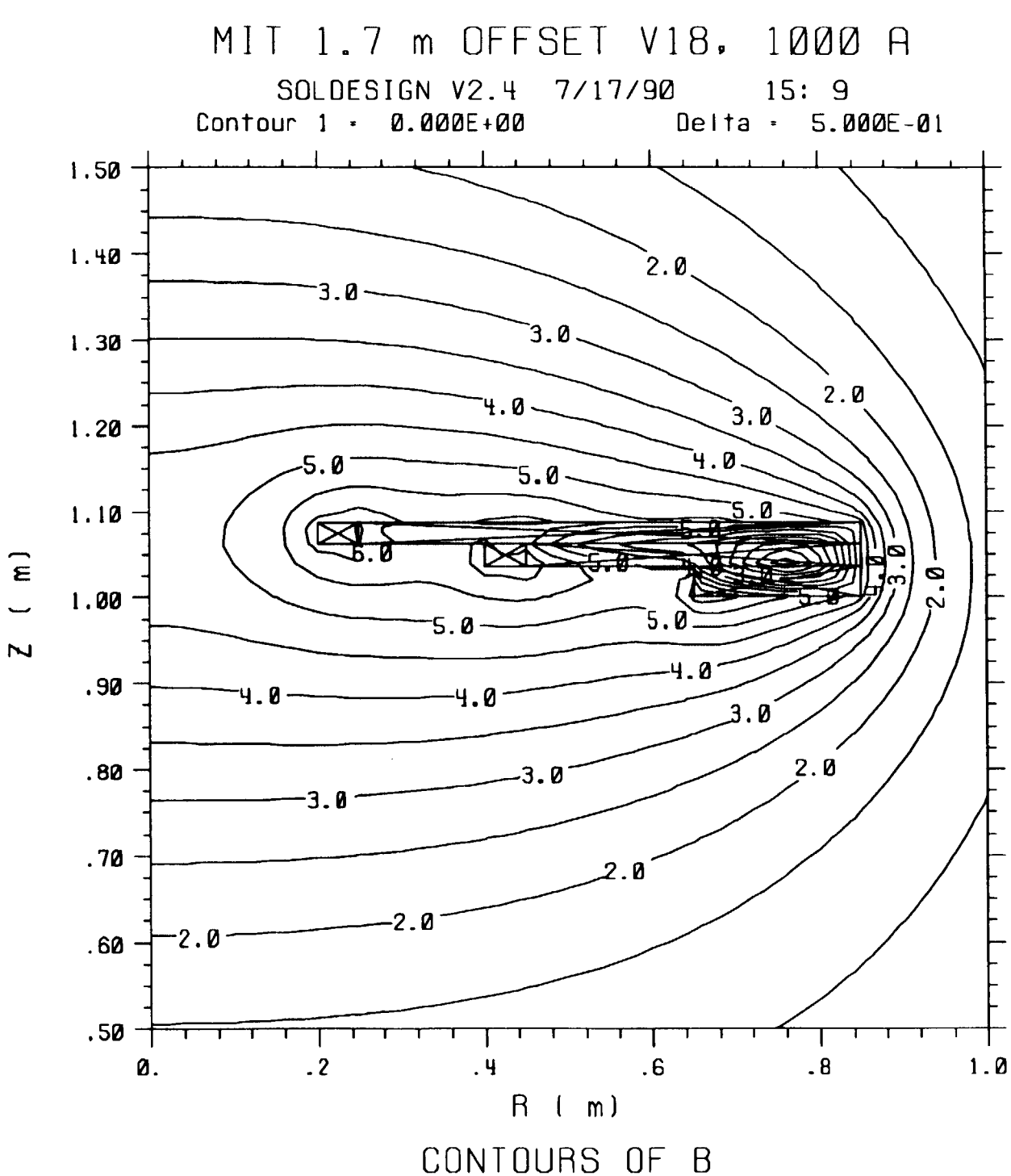

CONTOURS OF B

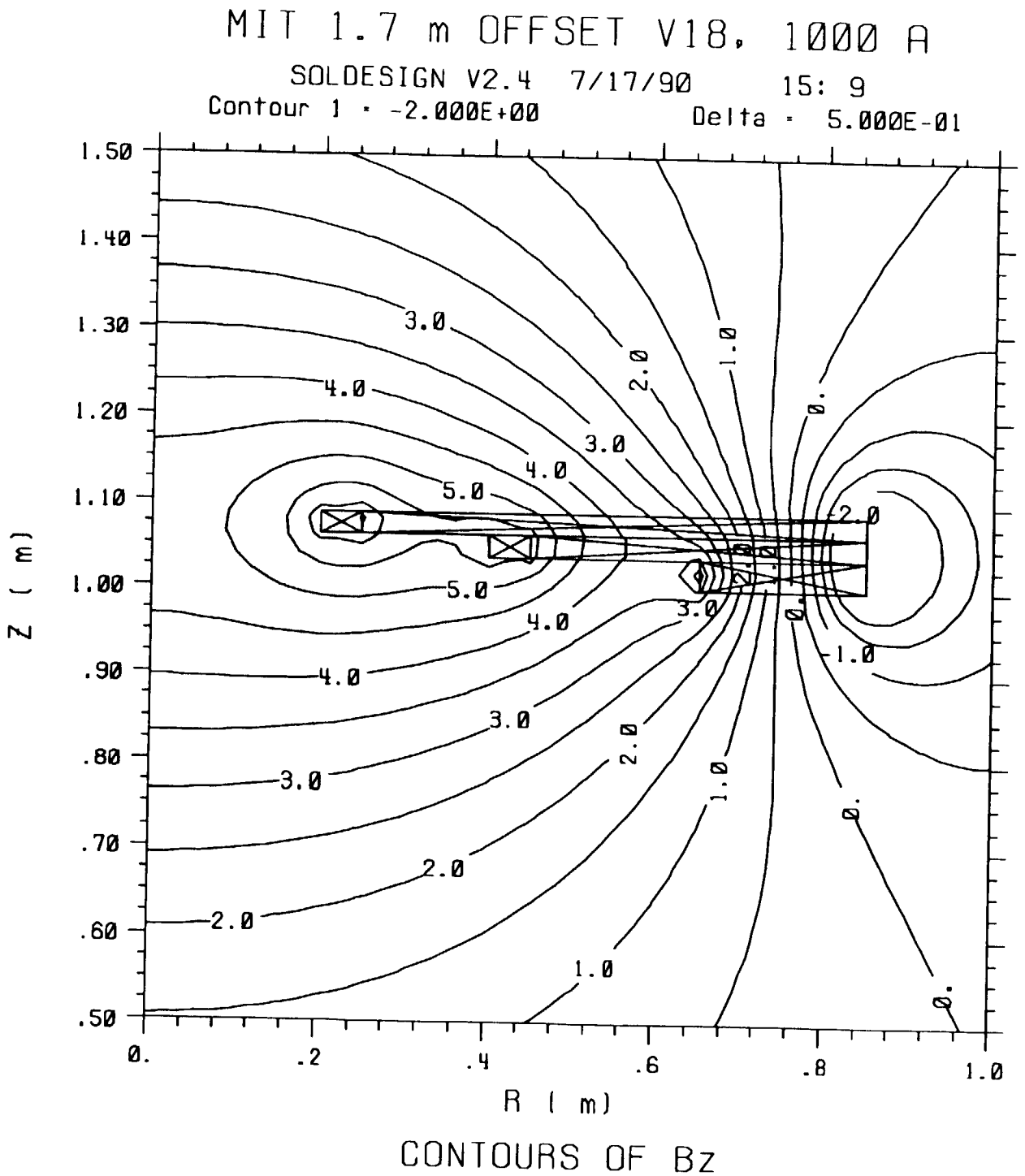

CONTOURS OF Bz

MIT 1.7 m VARIABLE PITCH R5

SOLDESIGN V2.4 7/10/90 16:37

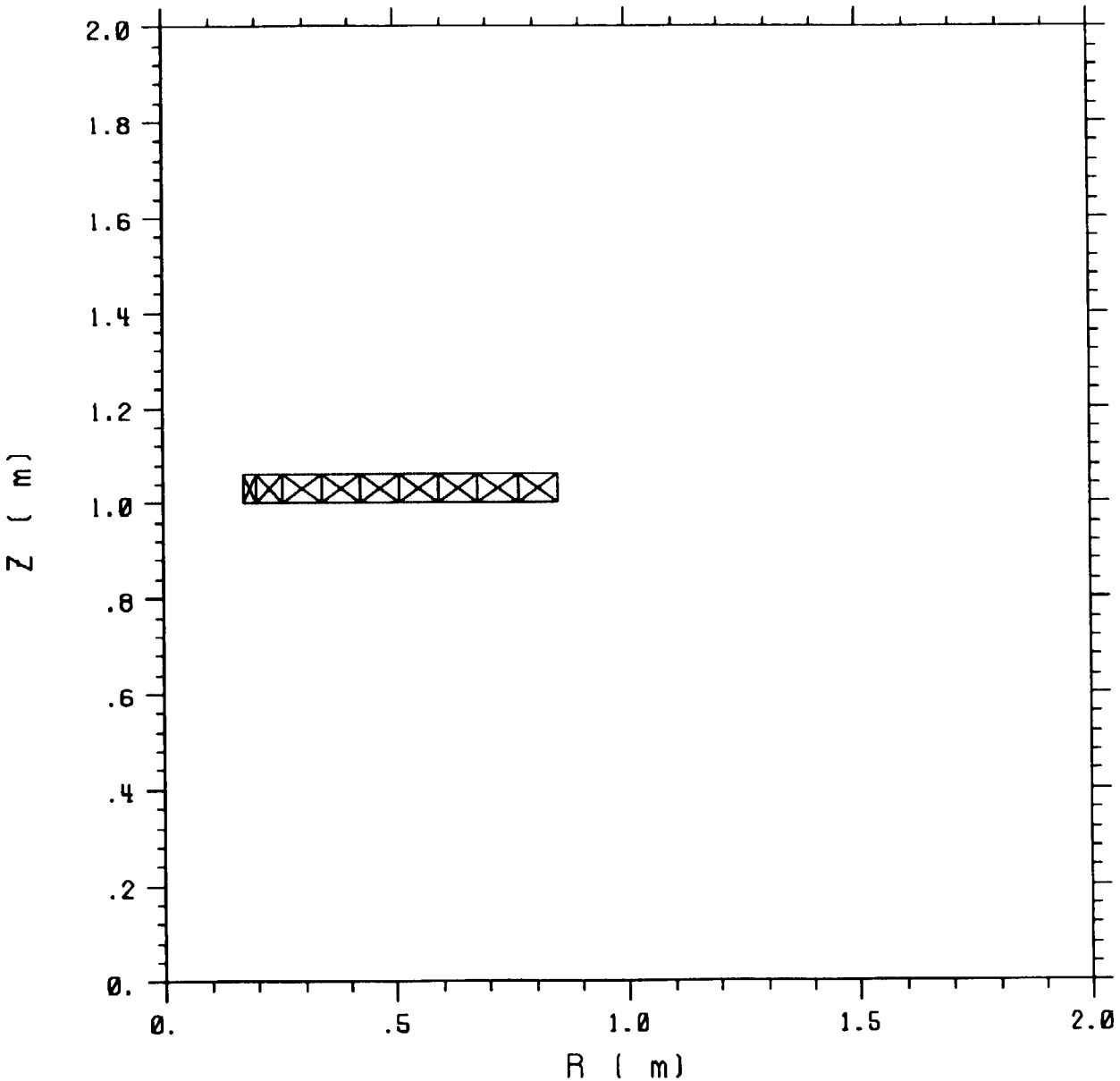

COILS

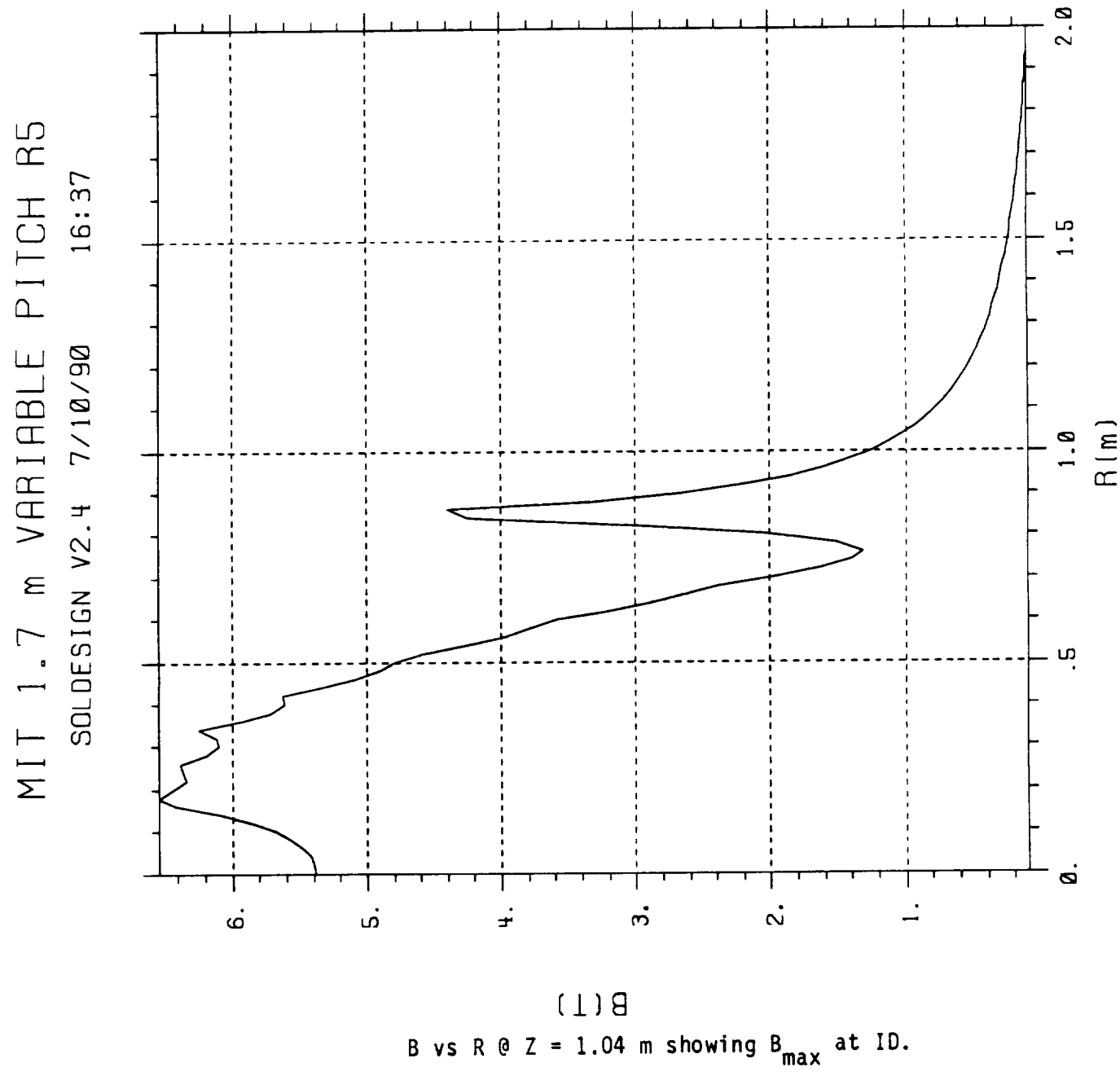

B vs R @ Z = 1.04 m showing B_{max} at ID.

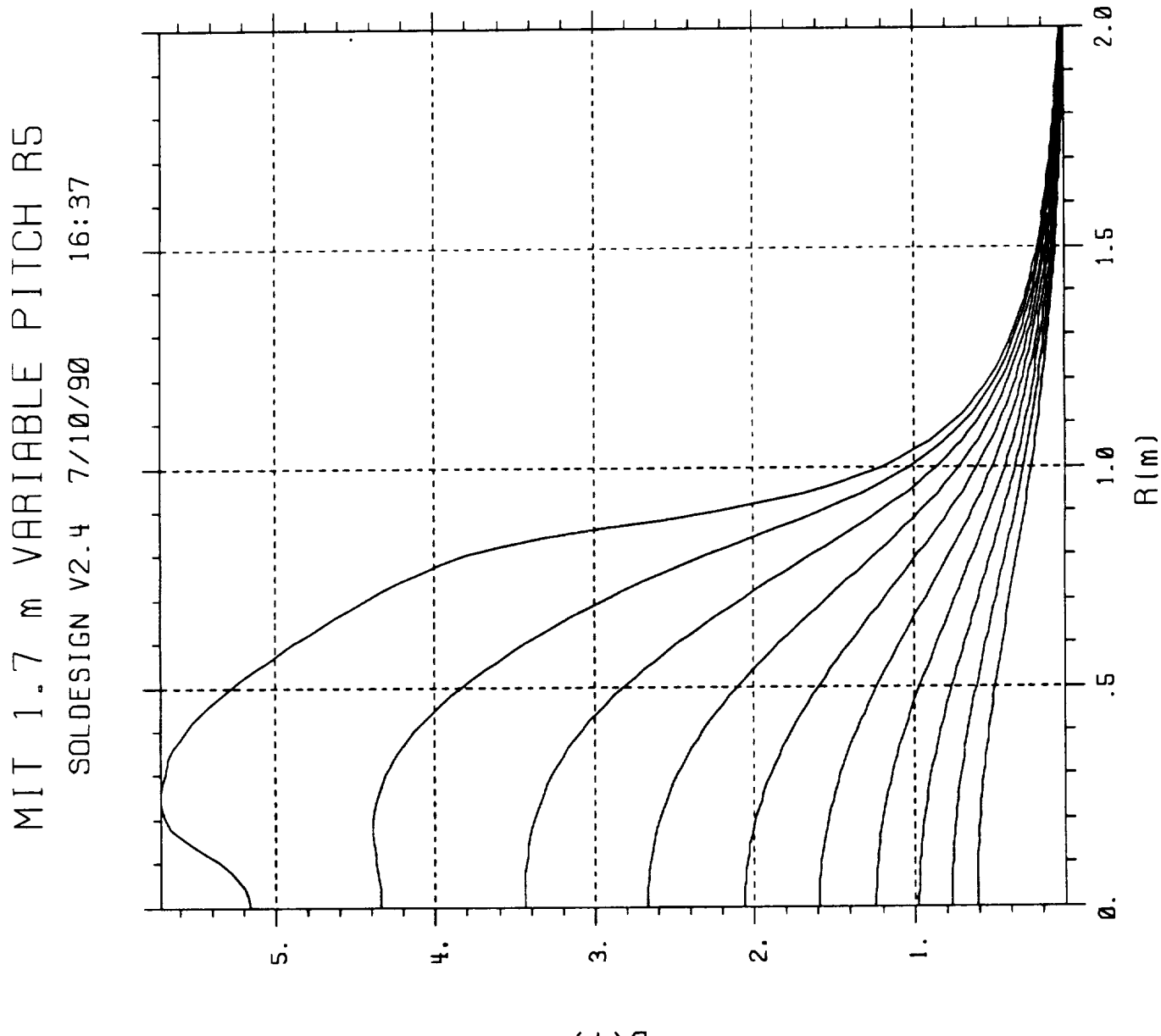

B vs R, with ΔZ = 10 cm. First (uppermost) curve @ Z = 1.1 m.

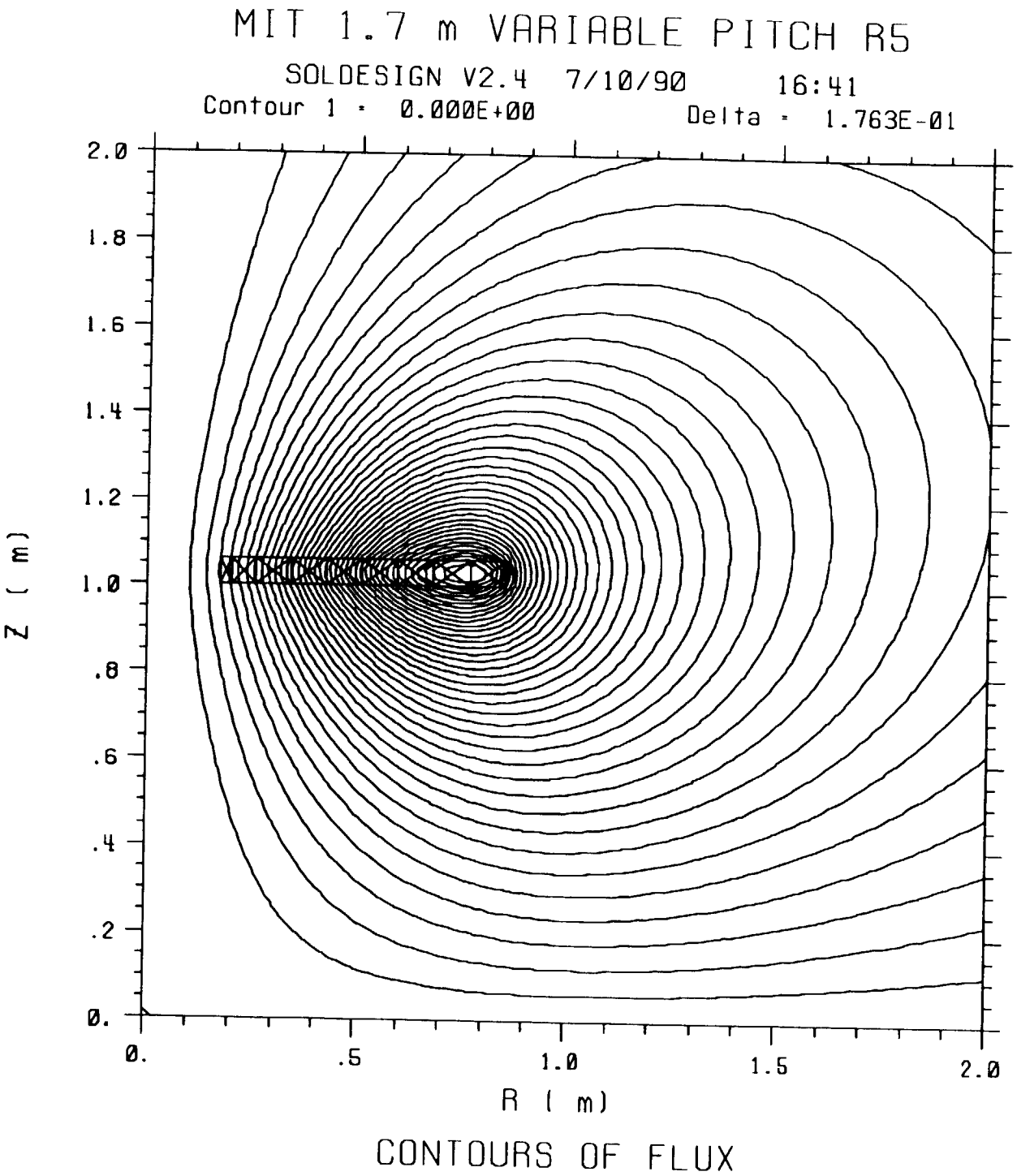

CONTOURS OF FLUX

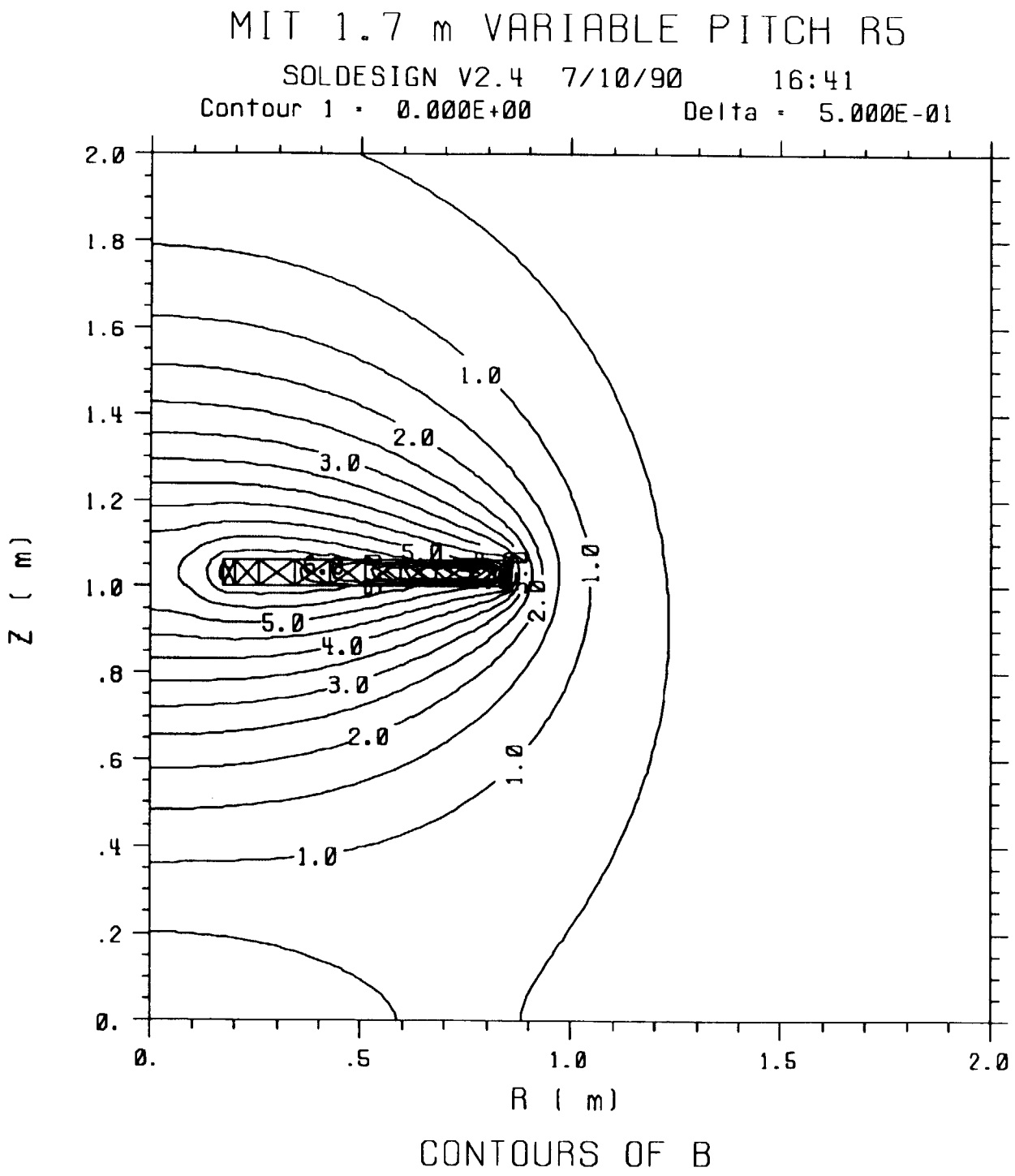
MIT 1.7 m VARIABLE PITCH R5
SOLDESIGN V2.4 7/10/90 16:41
Contour 1 = 0.000E+00 Delta = 5.000E-01
2.0
1.8
1.6
1.4
1.2
1.0
.8
.6
.4
.2
0.
Z (m)
0.
.5
1.0
1.5
2.0
R (m)
1.0
2.0
3.0
5.0
4.0
CONTOURS OF B

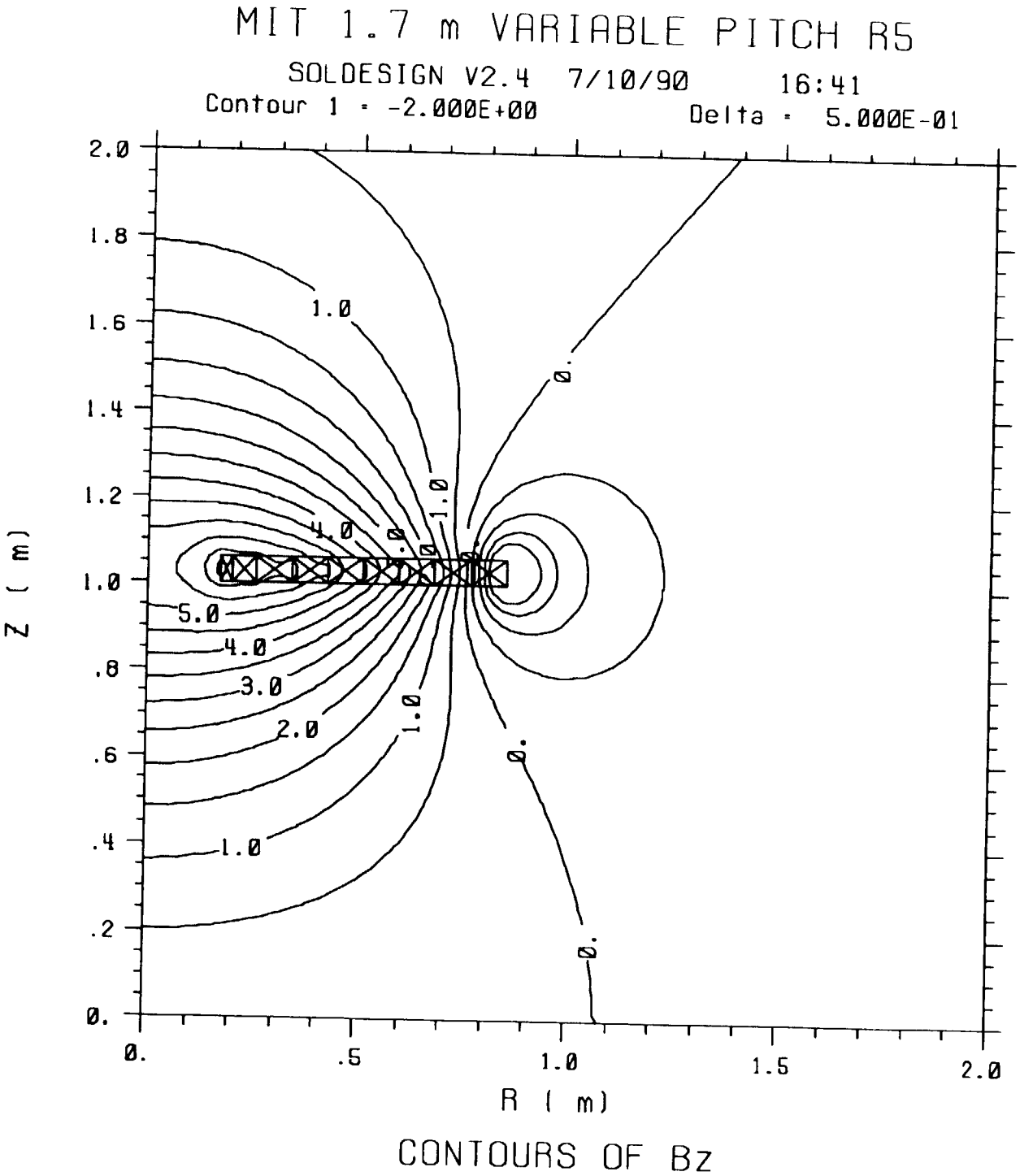

CONTOURS OF Bz

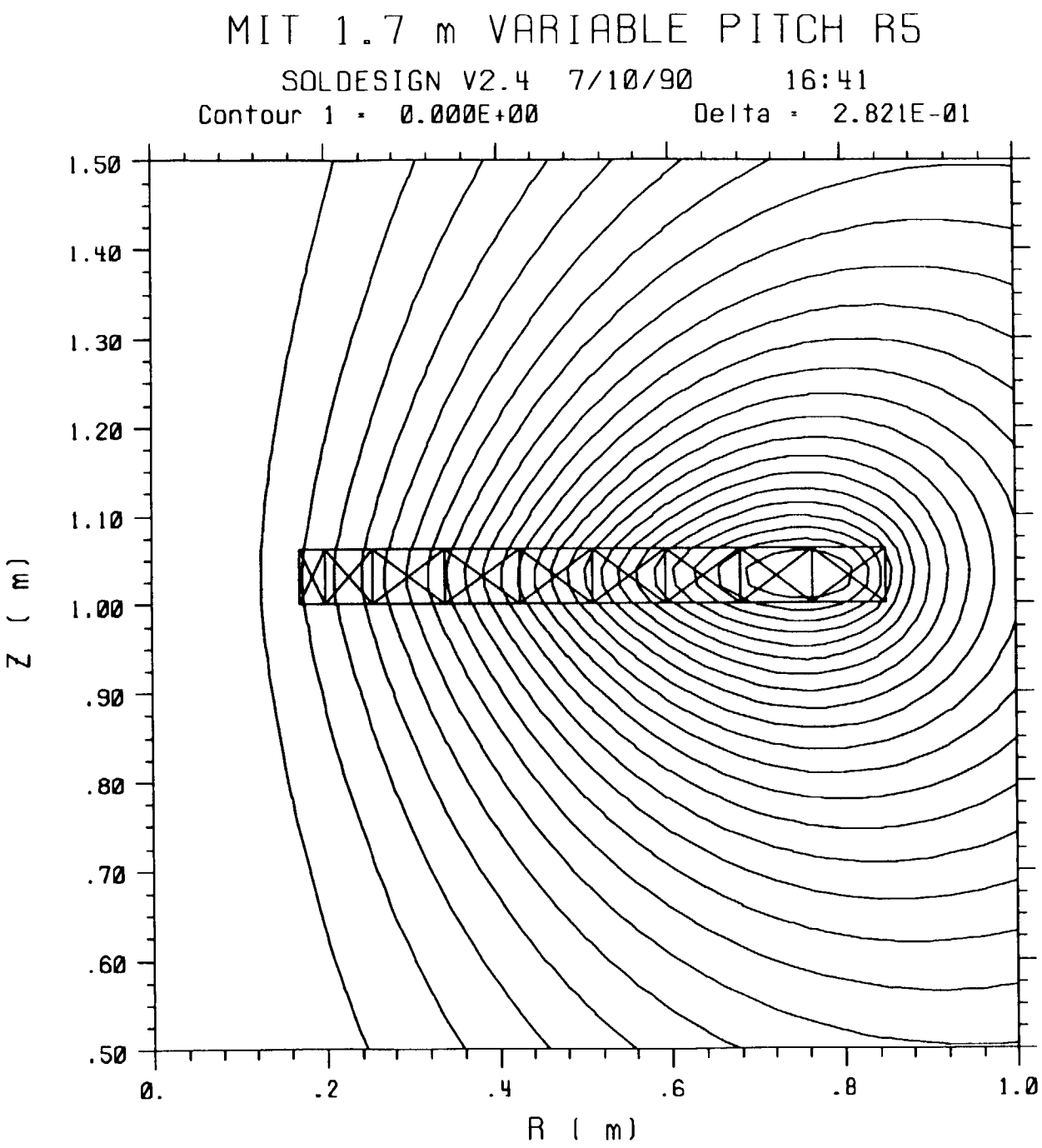

CONTOURS OF FLUX

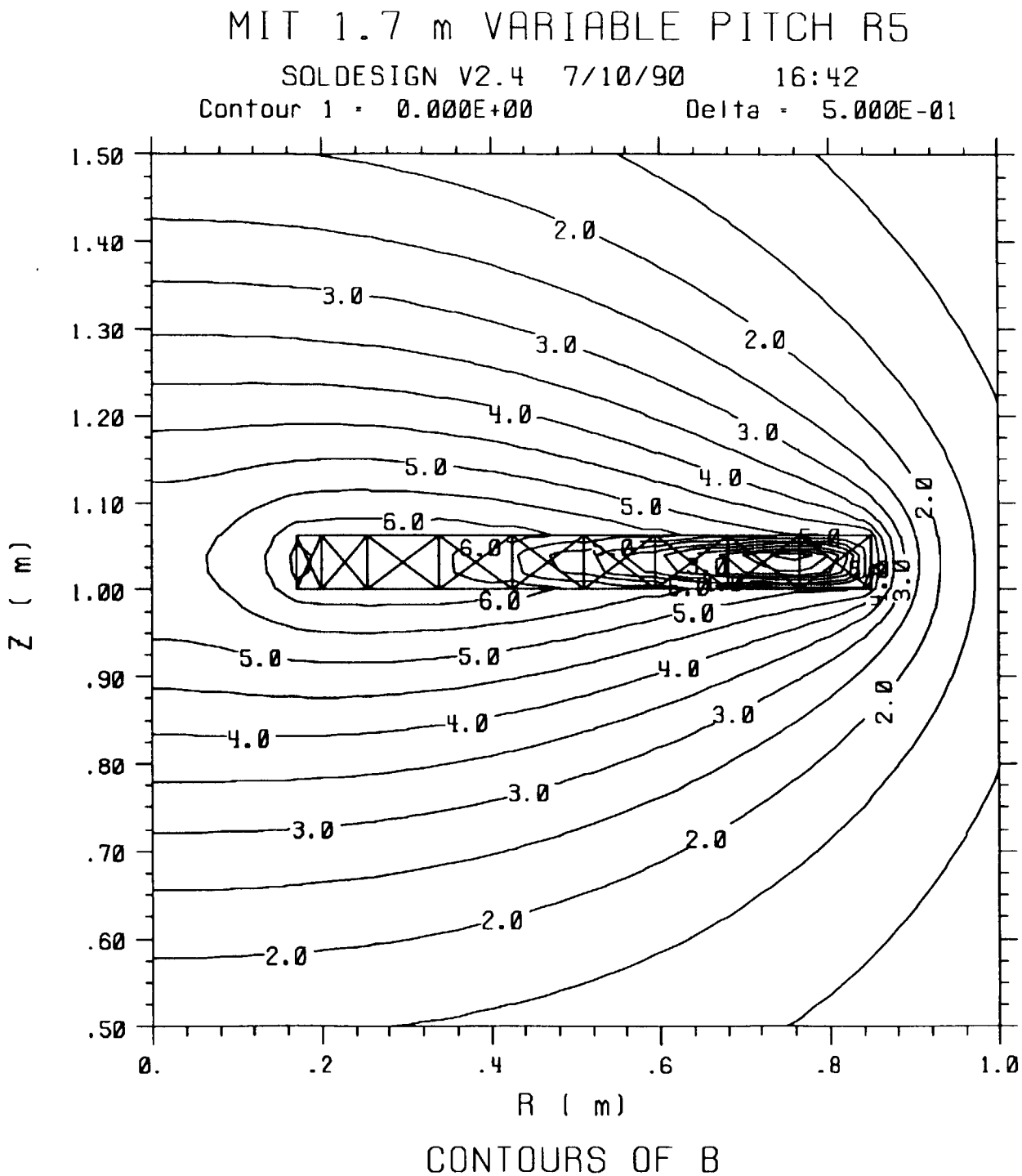

CONTOURS OF B

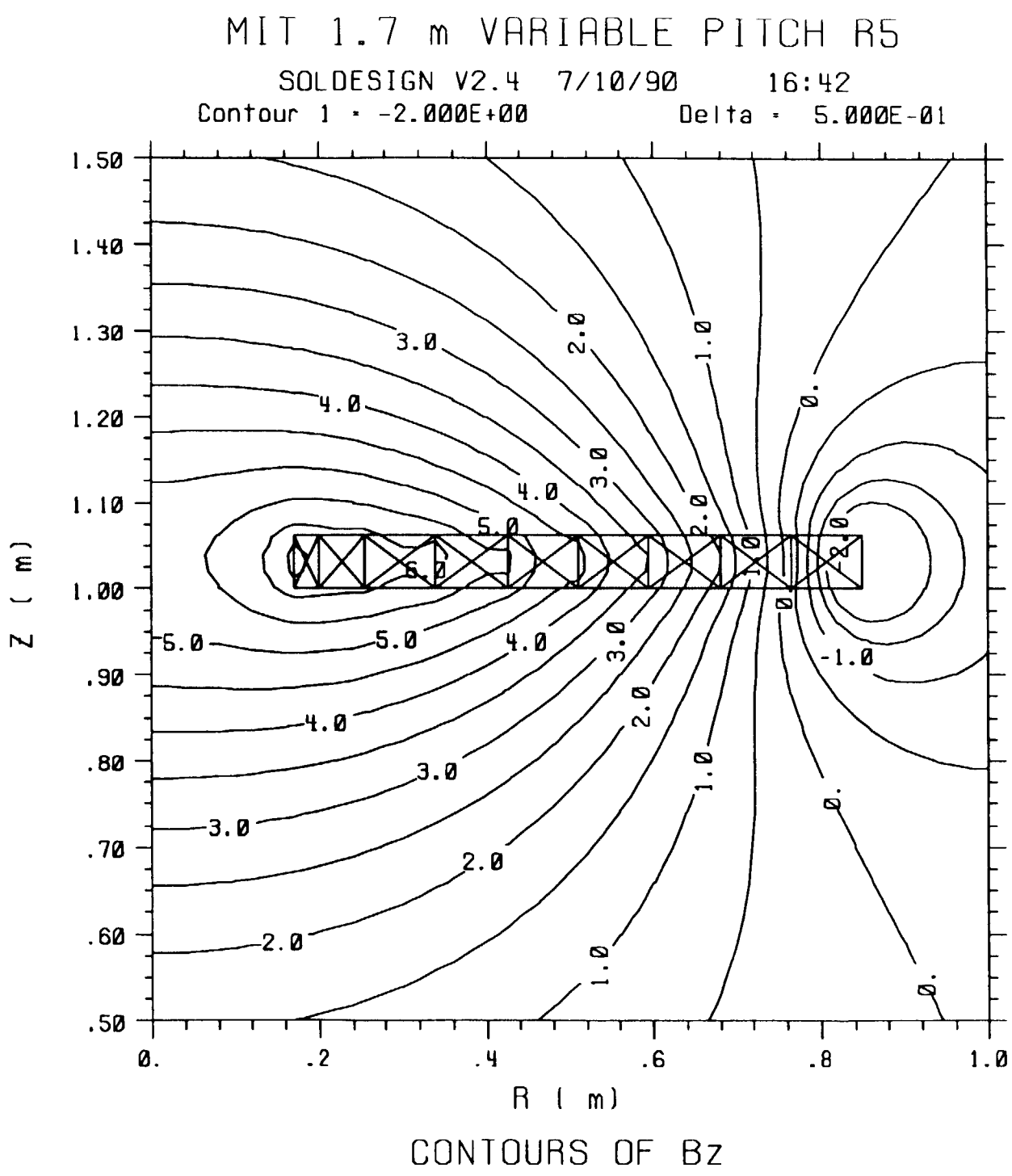
MIT 1.7 m VARIABLE PITCH R5
SOLDESIGN V2.4 7/10/90 16:42
Contour 1 = -2.000E+00 Delta = 5.000E-01
Z (m)
R (m)
1.50
1.40
1.30
1.20
1.10
1.00
.90
.80
.70
.60
.50
0.
.2
.4
.6
.8
1.0
CONTOURS OF Bz

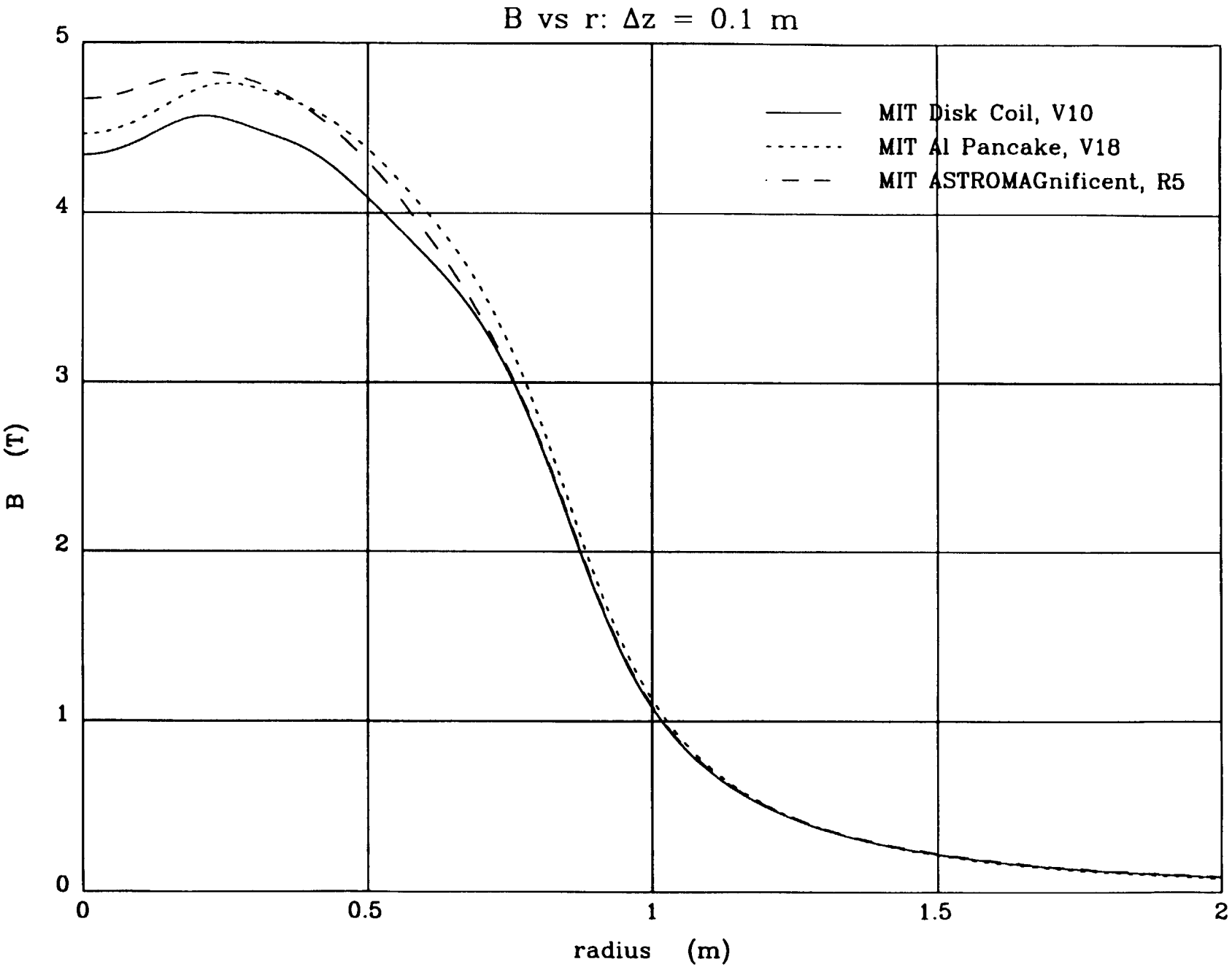
B vs r: Δz = 0.1 m
MIT Disk Coil, V10
MIT Al Pancake, V18
MIT ASTROMAGnificent, R5
B (T)
radius (m)
0
1
2
3
4
5
0
0.5
1
1.5
2

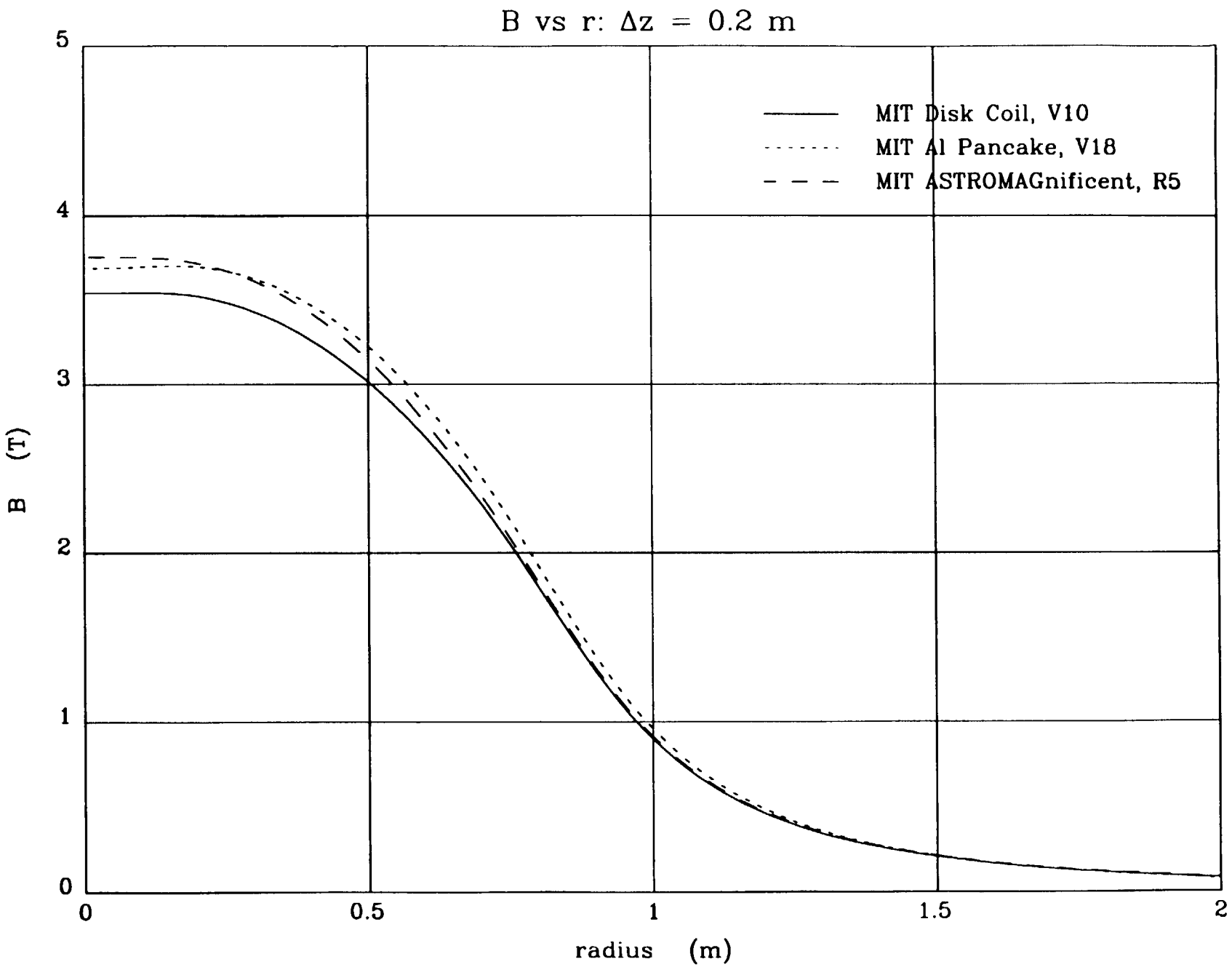
B vs r: Δz = 0.2 m
MIT Disk Coil, V10
MIT Al Pancake, V18
MIT ASTROMAGnificent, R5
B (T)
radius (m)
0
1
2
3
4
5
0
0.5
1
1.5
2

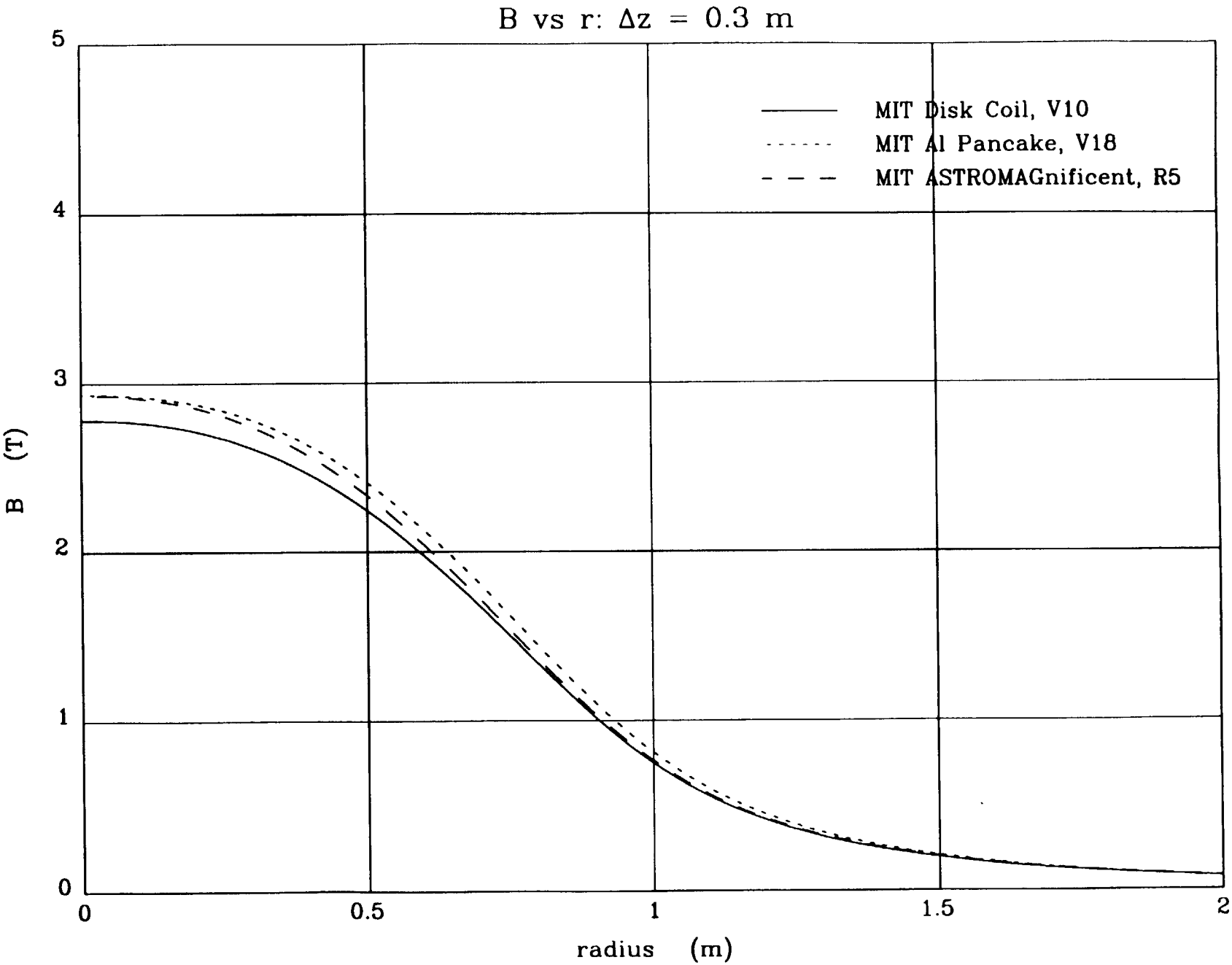
B vs r: Δz = 0.3 m
MIT Disk Coil, V10
MIT Al Pancake, V18
MIT ASTROMAGnificent, R5
B (T)
radius (m)
0
1
2
3
4
5
0
0.5
1
1.5
2

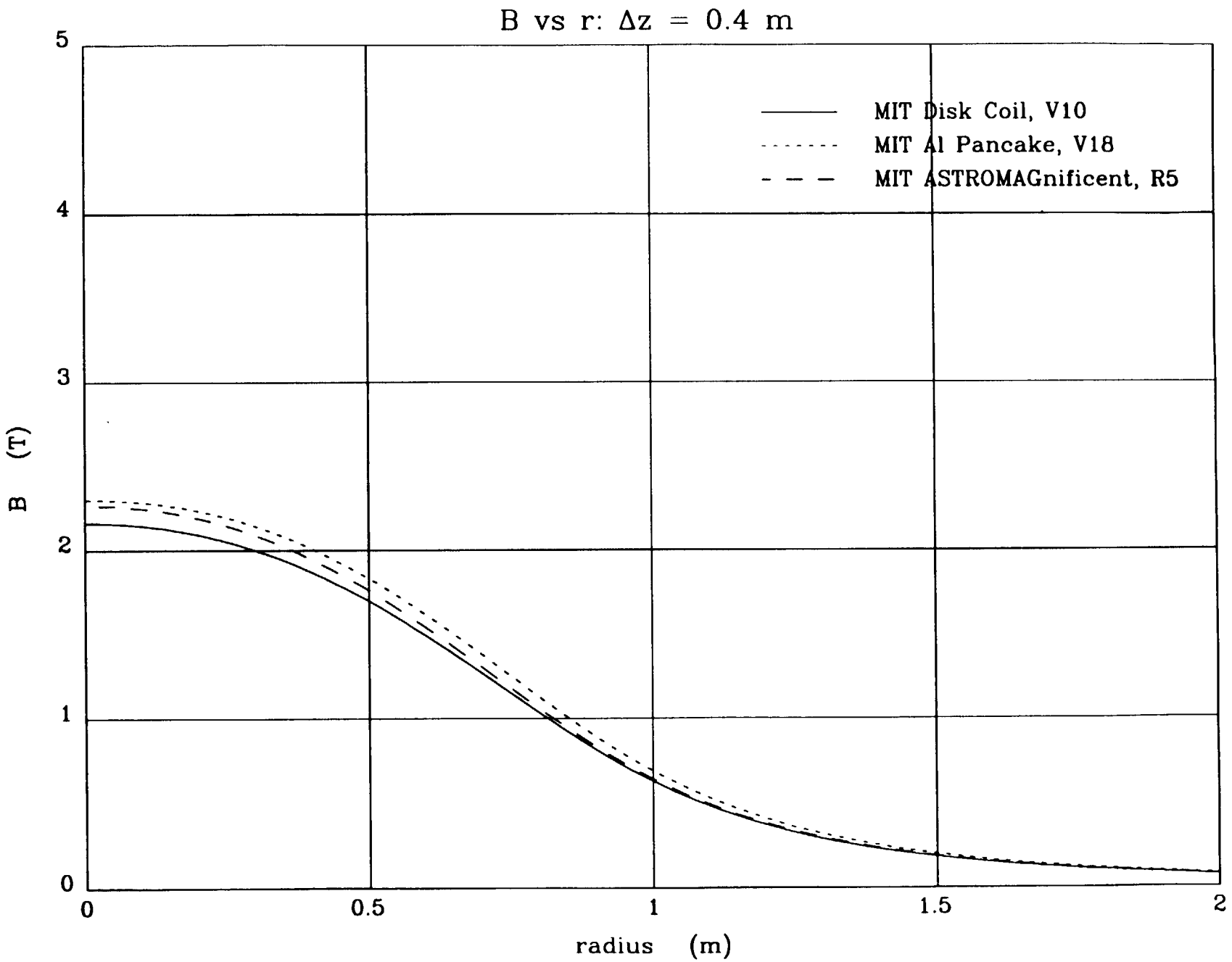
B vs r: Δz = 0.4 m
MIT Disk Coil, V10
MIT Al Pancake, V18
MIT ASTROMAGnificent, R5
B (T)
radius (m)
0
1
2
3
4
5
0
0.5
1
1.5
2

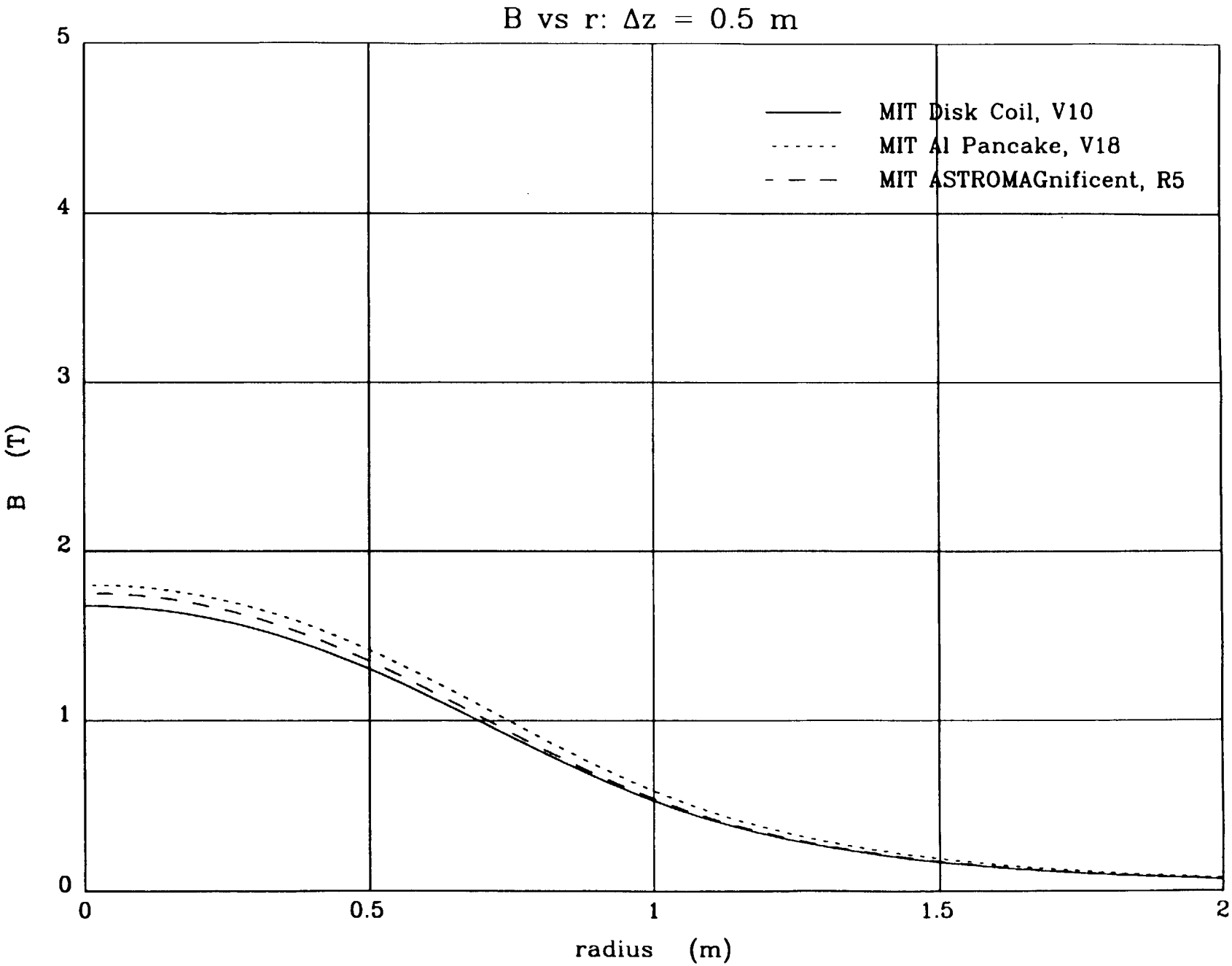
B vs r: Δz = 0.5 m
MIT Disk Coil, V10
MIT Al Pancake, V18
MIT ASTROMAGnificent, R5
B (T)
radius (m)
0
1
2
3
4
5
0
0.5
1
1.5
2

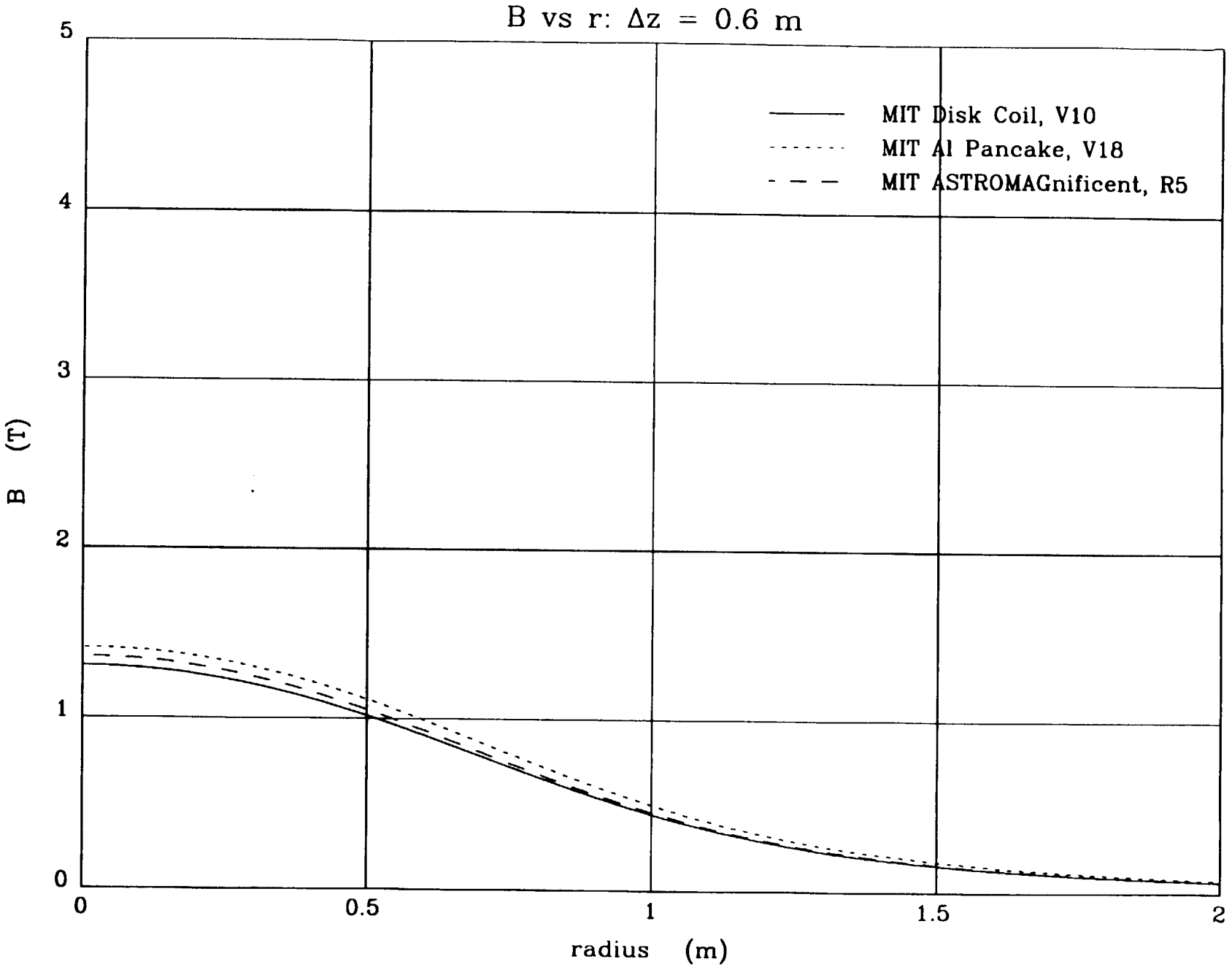
B vs r: Δz = 0.6 m
MIT Disk Coil, V10
MIT Al Pancake, V18
MIT ASTROMAGnificent, R5
B (T)
radius (m)
0
1
2
3
4
5
0
0.5
1
1.5
2

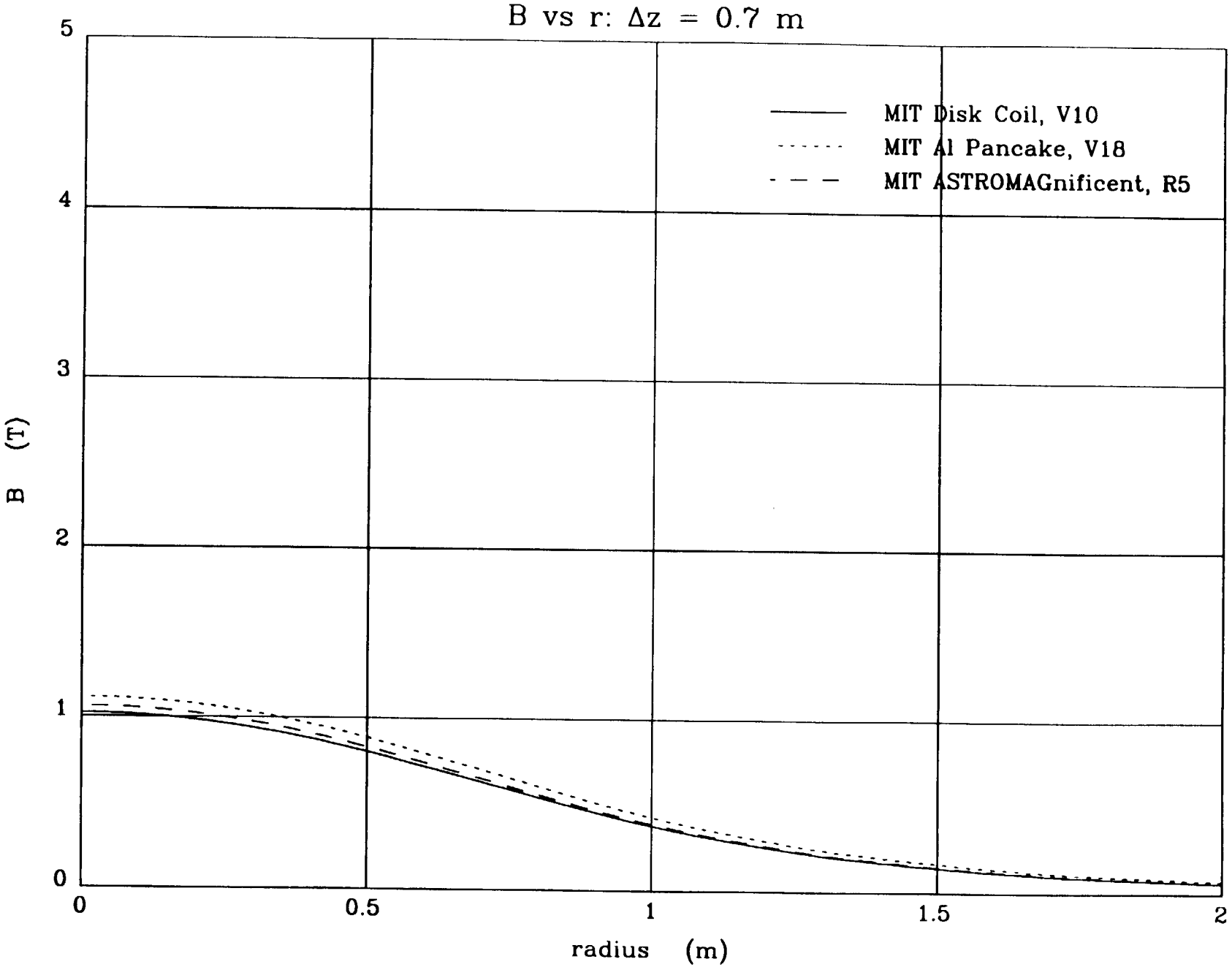
B vs r: Δz = 0.7 m
MIT Disk Coil, V10
MIT Al Pancake, V18
MIT ASTROMAGnificent, R5
B (T)
radius (m)
0
1
2
3
4
5
0
0.5
1
1.5
2

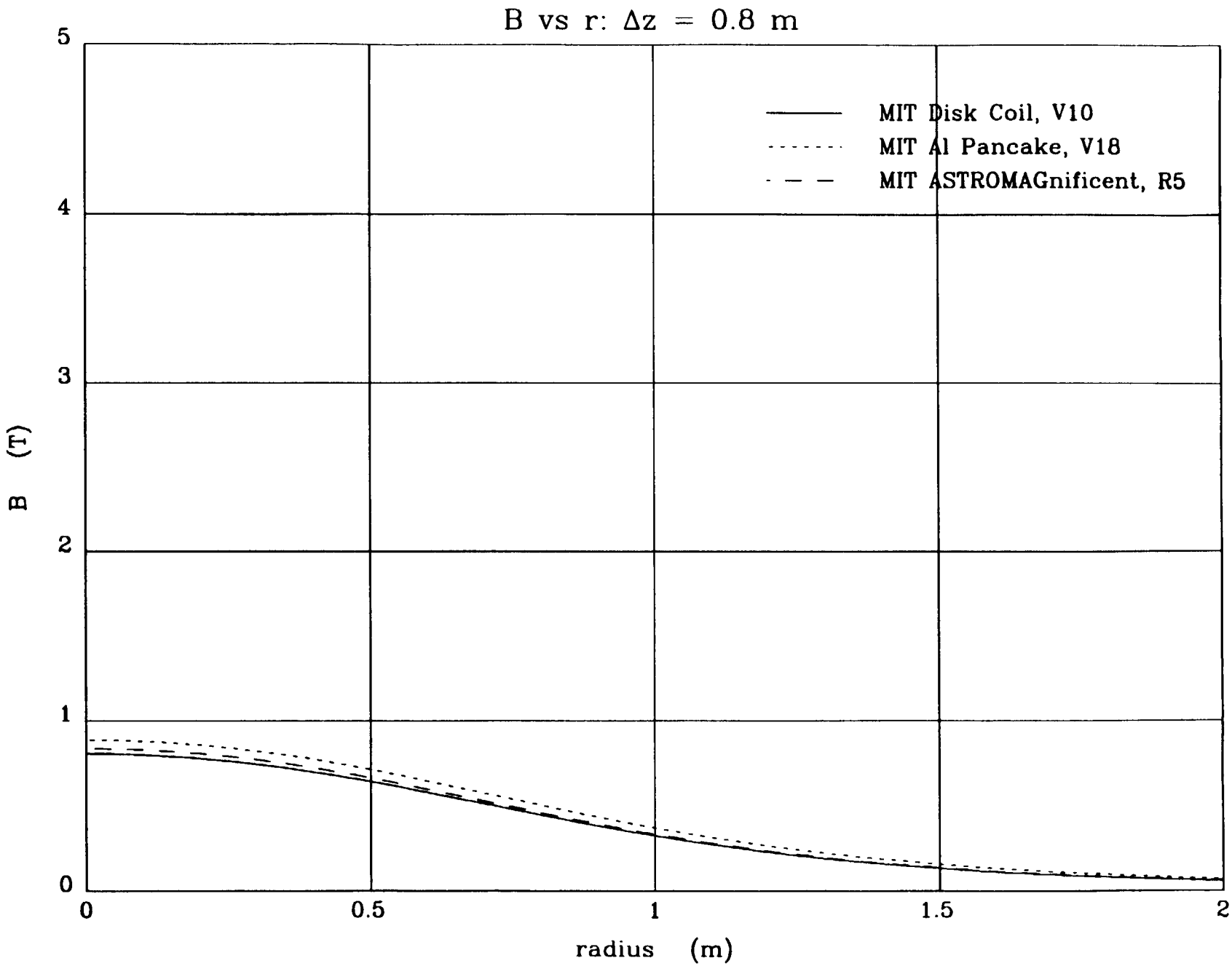
B vs r: Δz = 0.8 m
MIT Disk Coil, V10
MIT Al Pancake, V18
MIT ASTROMAGnificent, R5
B (T)
radius (m)
0
1
2
3
4
5
0
0.5
1
1.5
2

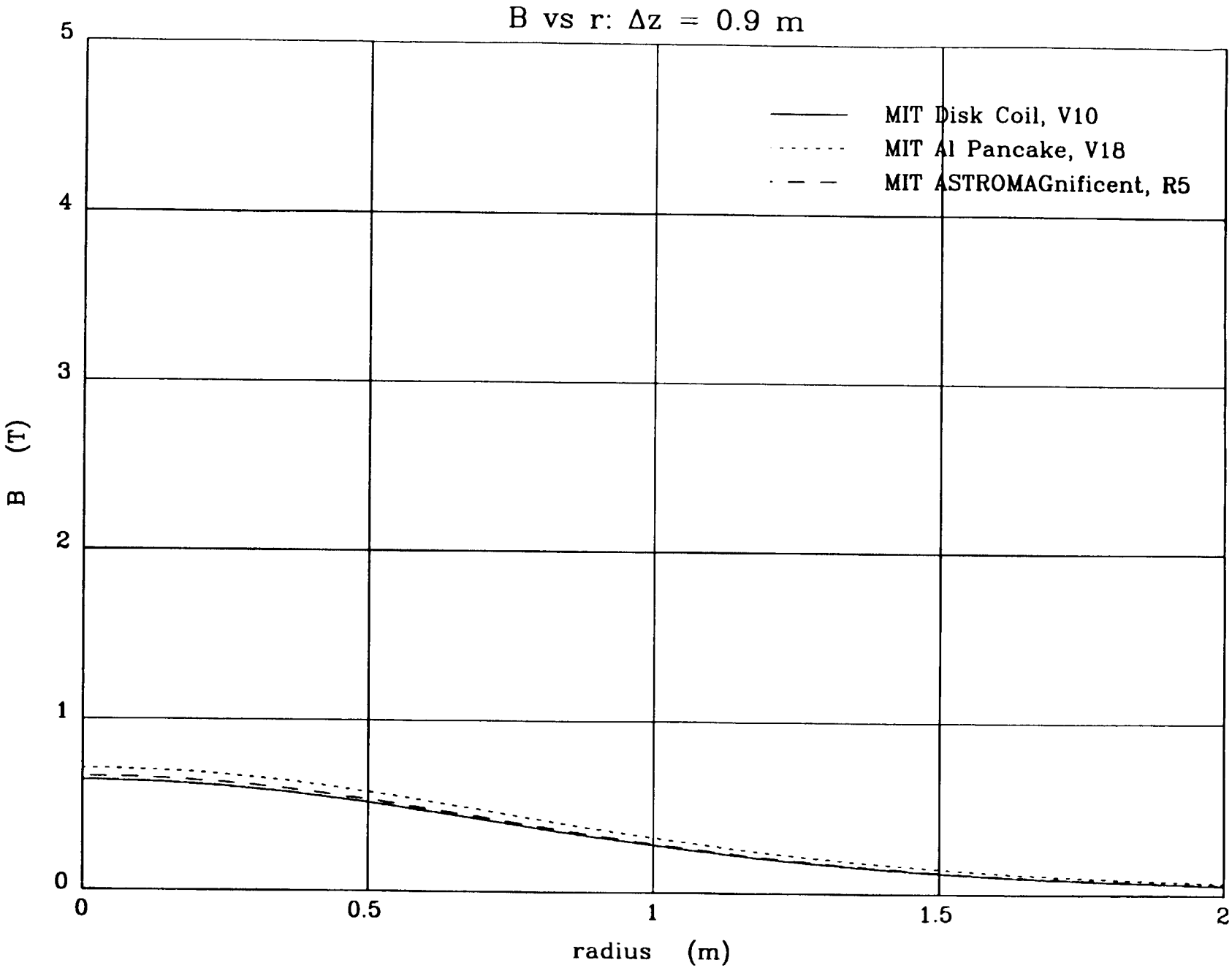
B vs r: Δz = 0.9 m
MIT Disk Coil, V10
MIT Al Pancake, V18
MIT ASTROMAGnificent, R5
B (T)
radius (m)
0
1
2
3
4
5
0
0.5
1
1.5
2

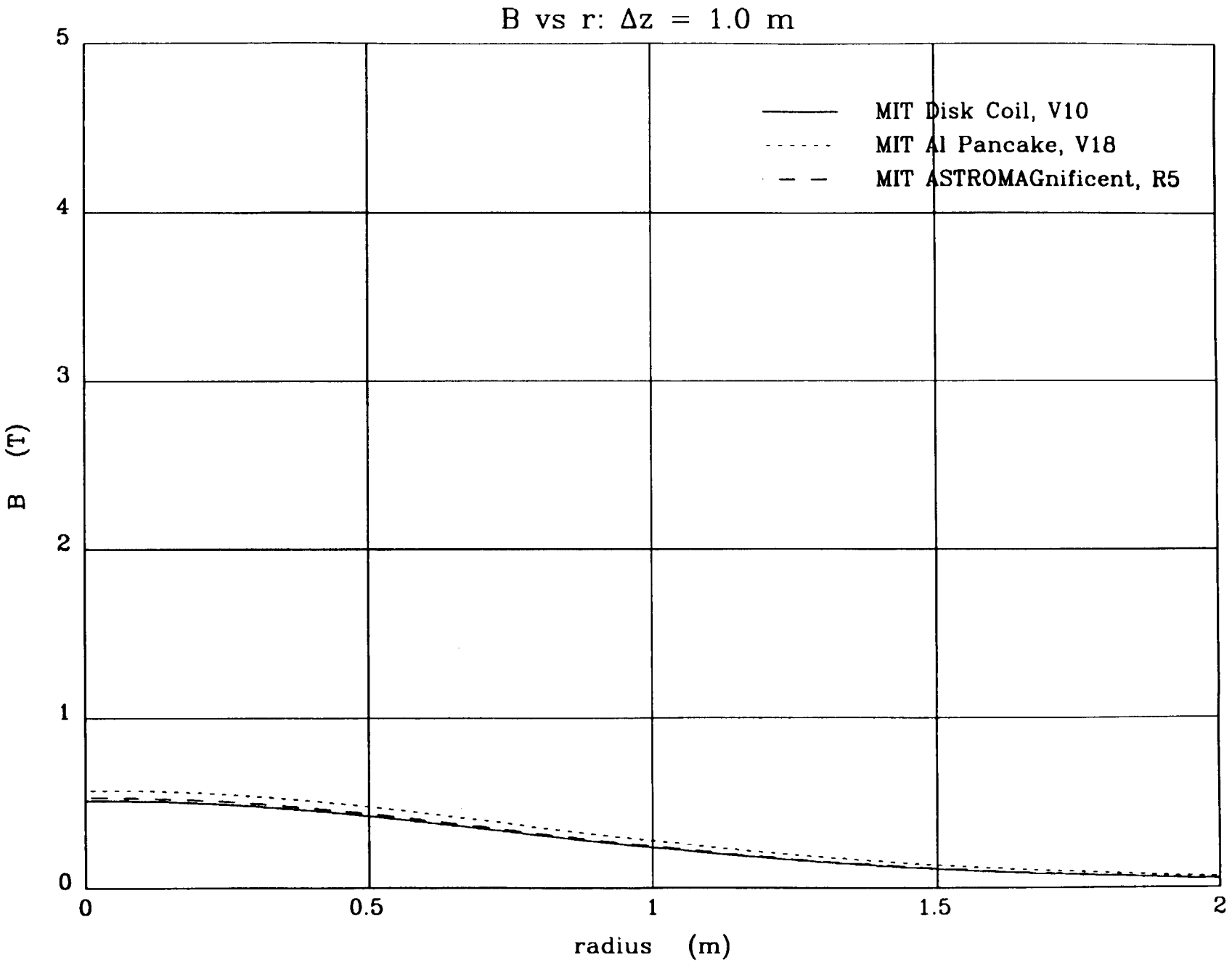
B vs r: Δz = 1.0 m
MIT Disk Coil, V10
MIT Al Pancake, V18
MIT ASTROMAGnificent, R5
B (T)
radius (m)
0
1
2
3
4
5
0
0.5
1
1.5
2

APPENDIX C

ASTROMAG PROTOTYPE TEST COIL

ASTROMAG PROTOTYPE TEST COIL

Description of Assembly

A magnet system comprised of a pair of self-supporting disk coils has been designed for the ASTROMAG facility. The coils are manufactured as a monolithic composite in which the superconductor wire is incorporated as one of the components. The proposed manufacturing process allows for the continuous winding of the coil thereby minimizing joints.

To evaluate and illustrate the manufacturing technique required to produce the two disk coils a subsize racetrack coil, shown in Fig. C.1, was manufactured. The following is an assembly description of the sequence of steps taken in the manufacturing process. This work was performed at A.I.T., Inc.

(1) The X-Y computer controlled wire feeding machine was set up with 0.0175" diameter superconductor wire. The wire has a wrap of kapton plus a proprietary epoxy bonding material to serve as an adhesive for winding.

(2) The graphite prepreg sheets had been cut into the desired size and stacked into layers composed of three plies of graphite/epoxy fabric and one unidirectional ply. To ensure adhesion of the wire during the winding, an additional two sheets of a proprietary B-stage epoxy were stacked on top.

(3) The first pancake contains a total of thirty (30) turns which were wound from the OD to the ID as shown in Fig. C.2. Next, a piece of graphite fabric was placed in the center and another at the perimeter of the pancake, Fig. C.3, to ensure a flat surface.

(4) The second set of graphite/epoxy with the same order and number of plies was placed on top of the pancake. The wire was fed through a cut in the plies and transferred to the top surface (Fig. C.4). Winding of the second pancake continued from the ID to the OD.

(5) Steps 3 and 4 were followed to complete the third and final pancake winding.

(6) The coil was then transported to MIT and prepared for a standard autoclave cure. Figure C.5 illustrates the curing cycle.

COMPARATIVE PERFORMANCE @ 13.8 MJ

	HEAO Al	DISK
MDR (TV)	3.43	4.35
$J\gamma$ (A/m^2)	1.6×10^8	1.27×10^8
σ (MPa)	260	100
$B_{max}P(T)$	6.97	5.6
I_{op} (A)	926	938
I_{op}/I_c	0.38	0.29
$E/_{mass}$ (J/g)	20	21(10-15 equiv.)

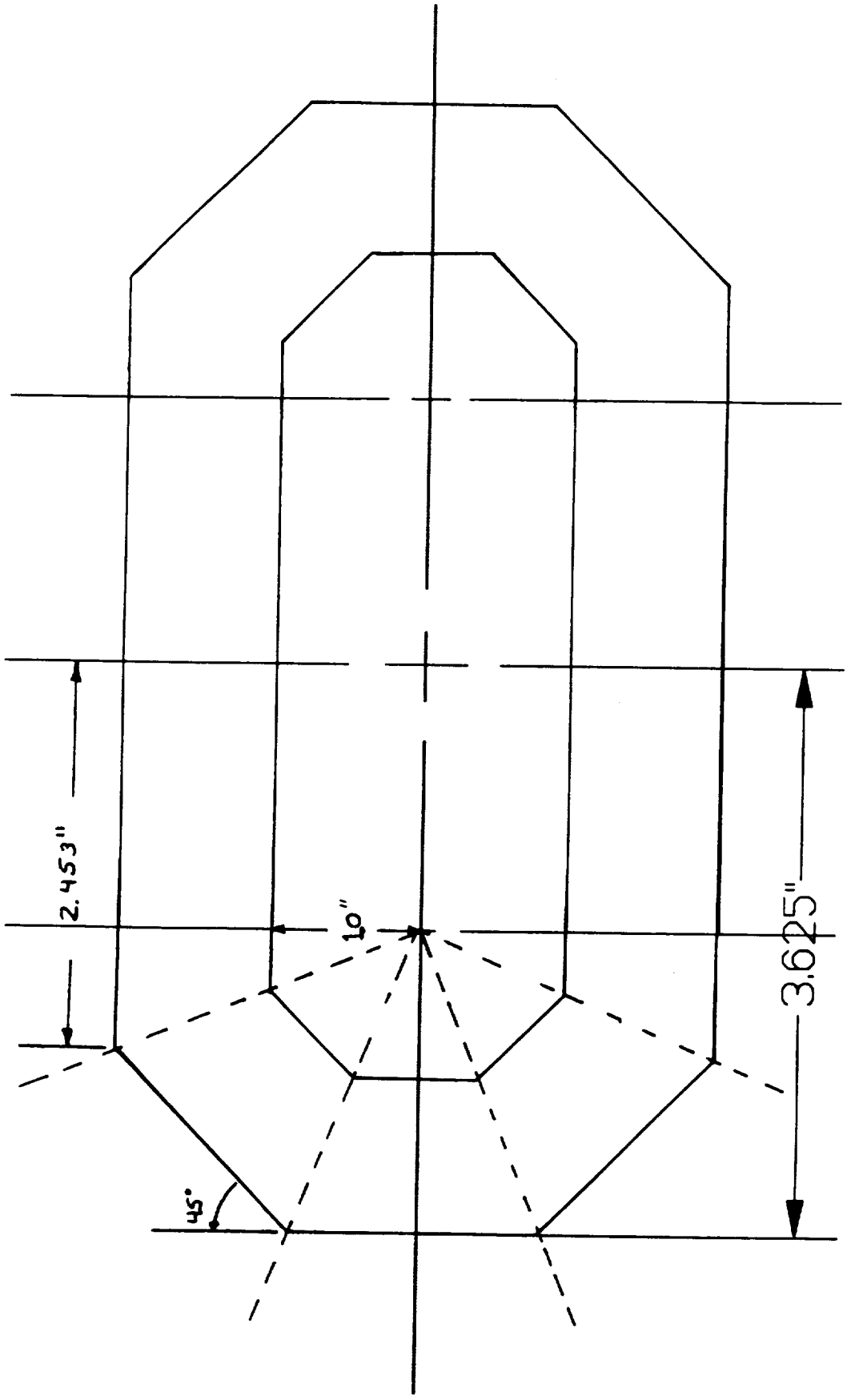

Figure C-1: Racetrack coil

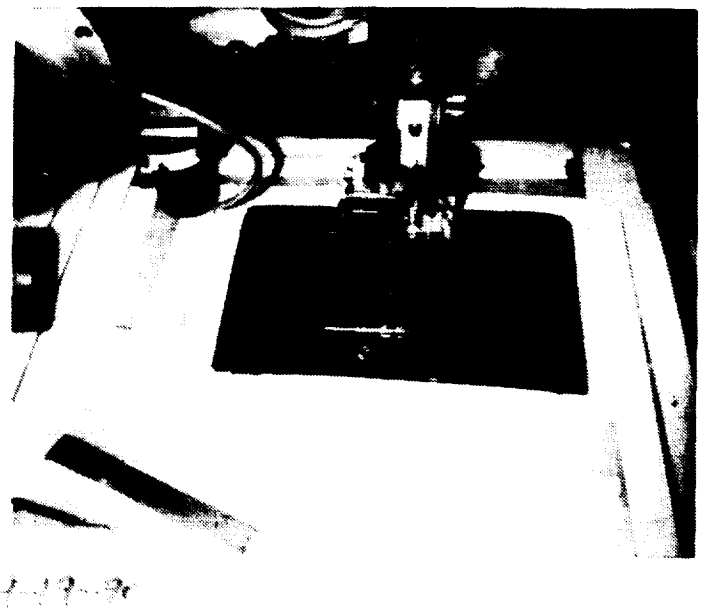

Figure C-2: Pancake winding from OD to ID

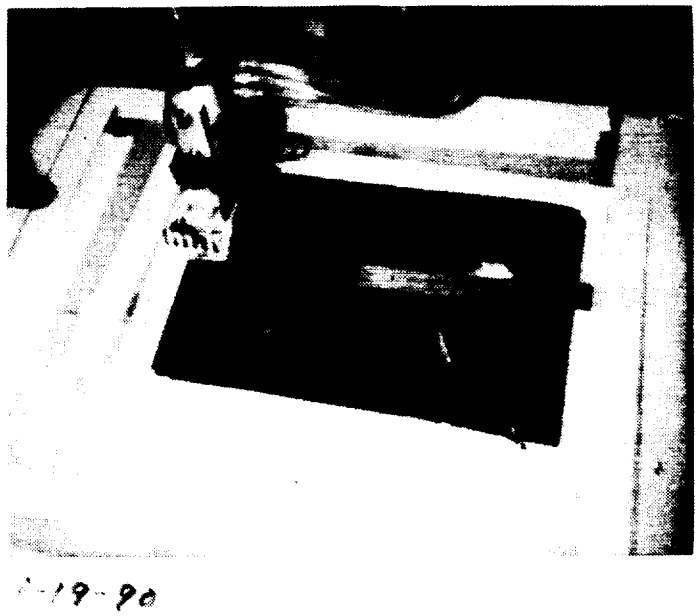

ORIGINAL PAGE
BLACK AND WHITE PHOTOGRAPH

Figure C-3: Graphite/epoxy fabric encasing the winding

ORIGINAL PAGE IS
OF POOR QUALITY

ORIGINAL PAGE IS
OF POOR QUALITY

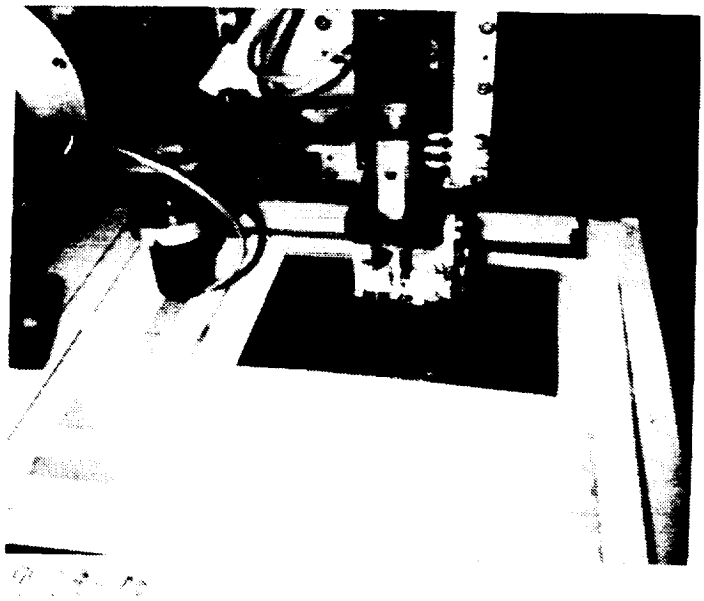

ORIGINAL PAGE
BLACK AND WHITE PHOTOGRAPH

Figure C-4: Transition point

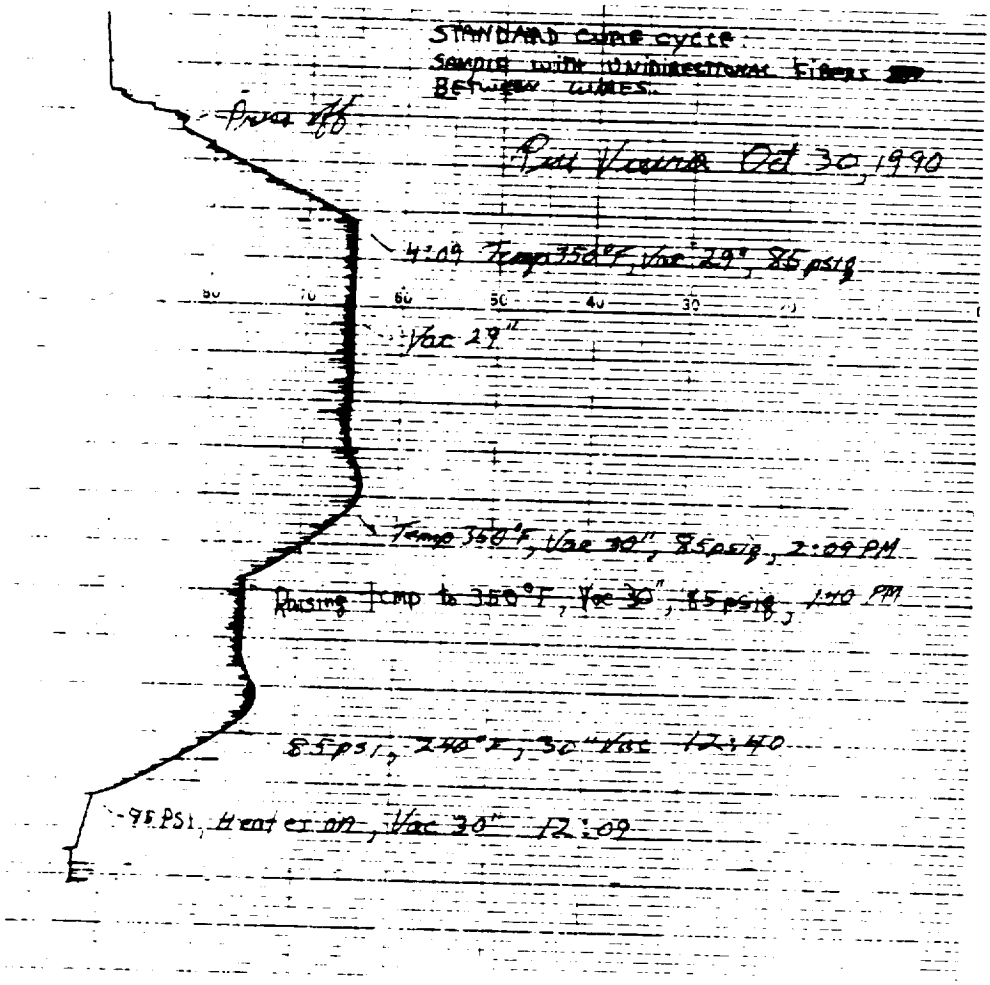

Figure C-5: Curing cycle